Kinetics and Mechanism of the Insertion of Olefins into Transition-Metal–Hydride Bonds[1]

Nancy M. Doherty and John E. Bercaw*

Contribution No. 7044 from the Arthur Amos Noyes Laboratory of Chemical Physics, California Institute of Technology, Pasadena, California 91125. *Received June 12, 1984*

Abstract: Permethylniobocene(III) olefin hydride complexes, $Cp^*_2Nb(CH_2{=}CHR)(H)$ ($Cp^* = \eta^5\text{-}C_5Me_5$), have been prepared by the reaction of $Cp^*_2NbH_3$ with the corresponding olefin (R = H, Ph, $p\text{-}Me_2NC_6H_4$, $p\text{-}MeOC_6H_4$, $p\text{-}MeC_6H_4$, $p\text{-}CF_3C_6H_4$) and by the reaction of $Cp^*_2NbCl_2$ with the corresponding alkyl Grignard reagent (R = H, Me). The product of migratory insertion of the olefin into the niobium–hydride bond is trapped by carbon monoxide or methyl isocyanide to give the permethylniobocene(III) alkyl carbonyl and methyl isocyanide derivatives, $Cp^*_2Nb(CH_2CH_2R)(L)$. The kinetics of the hydride–olefin insertion have been studied by ^1H NMR spectroscopy using magnetization transfer and coalescence techniques. Ground-state effects of olefin coordination were assessed by examining equilibria for competitive binding of ethylene and olefin ($CH_2{=}CHR$, R ≠ H) to $[Cp^*_2NbH]$. The data indicate that steric and electronic effects compete in the ground state. The mechanism of olefin insertion into the Nb–H bond is discussed in terms of a model involving a concerted cyclic four-center transition state. Electronic effects are found to dominate in the transition state and indicate the development of partial positive charge at the β carbon with the hydride moving as H^-, although the best linear free energy fit of the rate of insertion for the para-substituted styrenes indicates a rather modest value of −0.64 for ρ. Kinetic and thermodynamic isotope effects support the proposed model.

Olefin insertion into a metal–hydride bond and the related β-hydrogen elimination from a metal alkyl are fundamental transformations in organometallic chemistry. For elements as diverse as electron-deficient boron(III)[2] and electron-rich platinum(II)[3] reversible addition of a metal hydride to a carbon–carbon double bond is observed. Furthermore, both olefin insertion and β-hydrogen elimination are requisite steps in a variety of important catalytic reactions.[4] Thus, a detailed understanding of the mechanism of the olefin insertion/elimination process is of importance in both organometallic chemistry and catalysis.

Surprisingly, there is little quantitative information concerning the insertion of olefins into metal–hydrogen bonds or the microscopic reverse process, β-H elimination. Although many workers have performed kinetic studies on systems in which hydride–olefin insertion occurs, it has generally been observed that the insertion/elimination step is facile, reversible, and fast compared to other steps in the overall transformation.[5] Consequently, interpretation of the hydride–olefin insertion process in terms of the rates of the individual steps has proven difficult. In some cases, the kinetic data have been analyzed in terms of rate-limiting olefin insertion or β-H elimination.[6] Halpern and co-workers have measured the rate of insertion of cyclohexene into the rhodium–hydride bond during reaction of this olefin with $RhH_2Cl(PPh_3)_3$.[7a] Direct observations of reversible hydride–olefin insertion by dynamic NMR have been reported for several systems,[7b,c] and, although these experiments provide the order of magnitude for the rate of olefin insertion into metal–hydride bonds, activation parameters have not been derived and information on substituent effects is generally lacking.

Recently, using magnetization-transfer techniques, Roe[8a,b] has measured the activation parameters for intramolecular olefin insertion for *trans*-$HRh(C_2H_4)(PR_3)_2$ (R = isopropyl) by way of a *cis* intermediate. Moreover, Halpern and Okamoto have recently reported the rates of insertion of para-substituted styrenes into rhodium–hydride bonds.[8c]

Several features of the olefin insertion/β-H elimination process have been forwarded from the experimental data. Where product stereochemistry has been determined, net *cis* addition of M–H to the olefin is observed.[9] This finding has led to the proposal of a concerted, cyclic transition state. The dependence on ring size of the rate of thermal decomposition via β-H elimination of platinum(II) metallacycloalkanes[10] and the lack of β-H elimination from metal–norbornyl complexes[11] suggest the requirement of a planar arrangement of the four atoms (M–C–C–H) involved in bond making and bond breaking in the transition state for olefin insertion/β-H elimination. Additionally, coordination of the olefin to the metal center prior to insertion is generally assumed, at least for transition metals, with a *cis* relationship of the olefin and hydride ligands in the metal coordination sphere required.[4] From these observations, a general picture for olefin insertion and β-H elimination has emerged (eq 1).[12] Thus, insertion of olefin into a metal–hydrogen bond is usually described as a concerted intramolecular process involving a planar cyclic transition state with overall *cis* addition of M–H to the olefin double bond.[13]

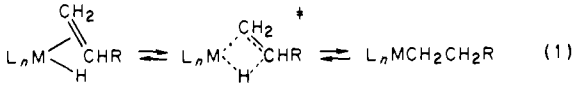

(1)

(1) A preliminary report of some of the material has appeared: McGrady, N. D.; McDade, C.; Bercaw, J. E. In "Organometallic Compounds: Synthesis, Structure, and Theory"; Shapiro, B. L., Ed.; Texas A&M University Press: College Station, TX, 1983; pp 46–85.

(2) Brown, H. C.; Zweifel, G. *J. Am. Chem. Soc.* **1966**, *88*, 1433–1439.

(3) Chatt, J.; Coffey, R. S.; Gough, A.; Thompson, D. T. *J. Chem. Soc. A* **1968**, 190–194.

(4) See, for example: Parshall, G. W. "Homogeneous Catalysis"; Wiley: New York, 1980; Chapters 3–5.

(5) (a) Whitesides, G. M.; Gaasch, J. F.; Stredonsky, E. R. *J. Am. Chem. Soc.* **1972**, *94*, 5258–5270. (b) Reger, D. L.; Culbertson, E. C. *Ibid.* **1976**, *98*, 2789–2794. (c) Kazlauskas, R. J.; Wrighton, M. S. *Ibid.* **1982**, *104*, 6005–6015; *Organometallics* **1982**, *1*, 602–611. (d) Watson, P. L.; Roe, D. C. *J. Am. Chem. Soc.* **1982**, *104*, 6471–6473. (e) Komiya, S.; Morimato, Y.; Yamamoto, A.; Yamamoto, T. *Organometallics* **1982**, *11*, 1528–1536. (f) Ozawa, F.; Ito, T.; Yamamoto, A. *J. Am. Chem. Soc.* **1980**, *102*, 6457–6463.

(6) (a) Clark, H. C.; Jablonski, C. R. *Inorg. Chem.* **1974**, *13*, 2213–2218. (b) Ikariya, T.; Yamamoto, A. *J. Organomet. Chem.* **1976**, *120*, 257–284. (c) Evans, J.; Schwartz, J.; Urquhart, P. W. *Ibid.* **1974**, *81*, C37–C39.

(7) (a) Halpern, J.; Okamoto, T.; Zakchariev, A. *J. Mol. Catal.* **1976**, *2*, 65–68. (b) Byrne, J. W.; Blaser, H. U.; Osborn, J. A. *J. Am. Chem. Soc.* **1975**, *97*, 3871–3873. (c) Chaudret, B. N.; Cole-Hamilton, D. J.; Wilkinson, G. *Acta Chem. Scand., Ser. A* **1978**, *A32*, 763–769. (d) Pardy, R. A.; Taylor, M. J.; Constable, E. C.; Mersh, J. D.; Sanders, J. K. M. *J. Organomet. Chem.* **1982**, *231*, C25–C30.

(8) (a) Roe, D. C. XIth International Conference on Organometallic Chemistry, Callaway Gardens, Pine Mountain, Georgia, Oct 10–14, 1983, Abstracts, p 133. (b) Roe, D. C. *J. Am. Chem. Soc.* **1983**, *105*, 7771–7772. (c) Halpern, J.; Okamoto, T. *Inorg. Chim. Acta*, in press.

(9) (a) Labinger, J. A.; Hart, D. W.; Seibert, W. E., III; Schwartz, J. *J. Am. Chem. Soc.* **1975**, *97*, 3851–3852. (b) Nakamura, A.; Otsuka, S. *Ibid.* **1973**, *95*, 7262–7272. (c) The observation of *cis* metal-catalyzed olefin hydrogenation,[9d] which is presumed to involve an intermediate metal–alkyl complex, is also consistent with *cis* hydride–olefin insertion. (d) Collman, J. P.; Hegedus, L. S. "Principles and Applications of Organotransition Metal Chemistry"; University Science Books: Mill Valley, CA, 1980; Chapter 6 and references therein.

(10) McDermott, J. X.; White, J. F.; Whitesides, G. M. *J. Am. Chem. Soc.* **1976**, *98*, 6521–6528.

(11) Bower, B. K.; Tennent, H. G. *Ibid.* **1972**, *94*, 2512–2514.

(12) See, for example: ref 4, pp 29–31; ref 9d, pp 291–298; Henrici-Olivé, G.; Olivé, S. *Top. Curr. Chem.* **1976**, *67*, 107–127.

0002-7863/85/1507-2670$01.50/0

From these considerations, it can be seen that examination of the detailed mechanism of hydride–olefin insertion requires a system in which (1) the insertion step can be isolated for kinetic study from other steps in the overall reaction and (2) modification of the olefin and/or ligand environment can be achieved in order to determine substituent effects on the process. The permethylniobocene(III) olefin hydride derivatives, Cp^*_2Nb(olefin)(H) ($Cp^* = \eta^5$-C_5Me_5), proved nearly ideal for such a study. These complexes possess a controlled, well-defined ligand environment in which the olefin is coordinated to the metal center *cis* to the metal hydride with a planar arrangement of the olefin carbon–carbon and the metal–hydrogen bonds. Furthermore, these complexes are well-suited for dynamic NMR study. As a consequence of these properties of Cp^*_2Nb(olefin)H, the problems of rate-limiting ligand loss or addition as well as olefin rotation and isomerization in the metal–ligand sphere (e.g., cis ⇄ trans) are avoided. Finally, it has proven possible to prepare a series of substituted olefin complexes in order to examine the steric and electronic effects on the ground and transition states for olefin insertion. We report herein our findings for Cp^*_2Nb(olefin)(H).

Results

Synthesis and Characterization of Niobium Olefin Hydride Complexes. The reaction of $Cp^*_2NbH_3$ (**1**)[14] with excess ethylene at 90 °C in toluene or benzene results in the formation of $Cp^*_2Nb(CH_2{=}CH_2)(H)$ (**2**) (eq 2). This reaction is accom-

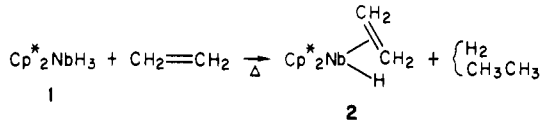

(2)

panied by the liberation of H_2 with slower production of ethane due to hydrogenation of excess ethylene.[14b] Compound **2** is isolated as a yellow crystalline solid in excellent yield (95%). A weak broad band at 1710 cm^{-1} in the infrared spectrum is assigned to the metal–hydride stretch (ν(Nb–D), 1238 cm^{-1}).

The ^1H NMR spectrum (90 and 500 MHz) for **2** in benzene-d_6 (Table I) consists of a singlet (δ 1.63) due to the pentamethylcyclopentadienyl ligands and a broad hydride resonance (δ −3.04). At 90 MHz an AA′BB′X (X = hydride) pattern is observed for the inequivalent ends of the ethylene ligand with the two complex pseudo-triplets centered at δ −0.23 and +0.65 (cf. Figure 1 for spectrum for **2** in toluene-d_8 at 25 °C). This spectrum is similar to the ^1H NMR spectra reported for the analogous complexes $Cp_2Nb(CH_2{=}CH_2)(H)$ and $Cp_2Nb(CH_2{=}CH_2)(CH_2CH_3)$.[15] At 500 MHz this NMR pattern simplifies to a triplet (δ −0.23) and a triplet of doublets (δ 0.65) with $J_{cis} = J_{trans} = 11$ Hz. The doublet splitting of the δ 0.65 resonance is due to coupling of these ethylene protons (which exchange with the hydride ligand; vide infra) to the hydride ($J_{HH} = 2$ Hz). This coupling is not resolved in the hydride resonance which is broadened significantly ($\nu_{1/2} = 7$ Hz) by interaction with the quadrupolar niobium nucleus ($I = {}^9/_2$). The ^{13}C NMR (125.8 MHz) spectrum for **2** (Table I) consists of a triplet (δ 20.8, $J_{CH} = 147$ Hz) and a triplet of doublets (δ 25.5, $J_{CH} = 150$ Hz, 6 Hz) for the ethylene carbons. The 6-Hz splitting of the resonance at δ 25.5 is due to coupling of one of the olefinic carbons to the hydride. Although it seems likely that the *endo* carbon is the one that is weakly coupled to the Nb–H proton, this is not unambiguously established.

The ^1H and ^{13}C NMR data, in particular the small value of the Nb–*H* to CH_2*C*H_2 coupling constant, are indicative of a "traditional" ethylene hydride ground-state structure, rather than

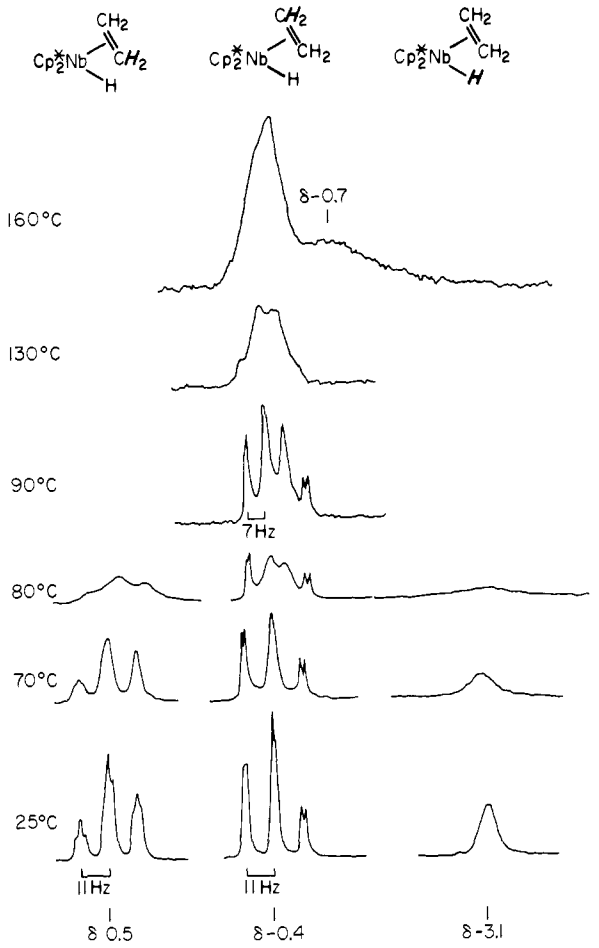

Figure 1. Variable-temperature ^1H NMR spectra for $Cp^*_2Nb(CH_2{=}CH_2)(H)$ (**2**) in toluene-d_8.

a niobium ethyl possessing an "agostic" Nb to C_β–H interaction.[16] Thus, by analogy to structurally characterized $Cp_2Nb(CH_2{=}CH_2)(CH_2CH_3)$, the geometry of **2** is as shown:

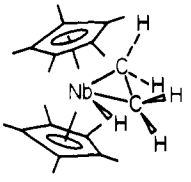

2

The olefin and hydride ligands are bonded in the equatorial plane of the bent metallocene, with the two olefinic carbons, the hydride ligand, and the metal atom coplanar.

Compound **2** can also be prepared by the reaction of $Cp^*_2NbCl_2$ (**3**)[14] with ethylmagnesium bromide in diethyl ether at 25 °C in moderate yield (eq 3). Two equivalents of the Grignard reagent

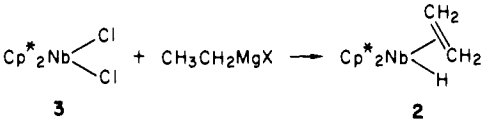

(3)

are required for this reaction. Presumably, 1 equiv acts as a reducing agent ($Nb^{IV} \rightarrow Nb^{III}$), the other as the source of an ethyl ligand which β-H eliminates to generate the olefin hydride complex. $Cp^*_2Nb(CH_2{=}CHMe)(H)$ (**4**) is prepared similarly by the reaction of **3** with excess *n*-propylmagnesium bromide (eq 4). Compound **4** is isolated as an orange crystalline solid, with the best yields (69%) obtained by using 3 equiv of $CH_3CH_2CH_2MgBr$.

(13) (a) Although concerted olefin insertion/elimination may best describe this reaction for a variety of organometallic systems, other pathways are possible. For example, Sweany and Halpern have shown that the reaction of $HMn(CO)_5$ with a sterically hindered olefin, $CH_2{=}C(CH_3)Ph$, proceeds via a radical pathway involving initial hydrogen atom abstraction by the olefin.[13b] (b) Sweany, R. L.; Halpern, J. *J. Am. Chem. Soc.* **1977**, *99*, 8335–8337.

(14) (a) Threlkel, R. S. Ph.D. Thesis, California Institute of Technology, 1980. (b) Cohen, S. A. Ph.D. Thesis, California Institute of Technology, 1982.

(15) Guggenberger, L. J.; Meakin, P.; Tebbe, F. N. *J. Am. Chem. Soc.* **1974**, *96*, 5420–5427.

(16) Brookhart, M.; Green, M. L. H. *J. Organomet. Chem.* **1983**, *250*, 395–408.

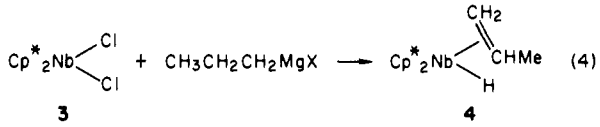

The reaction of **3** with $(CH_3)_2CHMgBr$ leads to a mixture of products containing some **4**. Similarly, attempts to prepare **4** by the reaction of **1** with propene resulted in an intractable mixture of products including **4** (^{1}H NMR).

The styrene and para-substituted styrene complexes (**5**) are prepared by the reaction of **1** with an excess of olefin (eq 5).

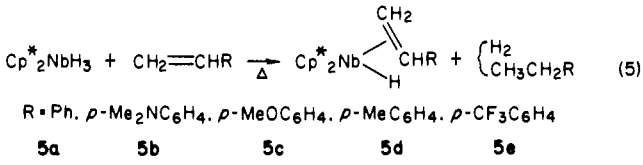

Production of H_2 and the corresponding para-substituted ethylbenzene is observed (^{1}H NMR). Good yields (50–80%) of the isolated yellow crystalline styrene complexes are obtained.

In contrast to the $Cp_2Nb(olefin)(H)$ ($Cp = \eta^5$-C_5H_5) complexes in which both *endo* and *exo* isomers are observed,[17] **4** and **5** are obtained in a single isomeric form. Models indicate that the endo isomer is sterically favored over the exo isomer:

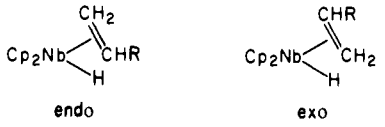

The observation of exchange of the hydride ligand with the hydrogen on the substituted end of the olefin (vide infra) support assignment of **4** and **5** as the endo isomers.

The ^{1}H NMR spectra (500 MHz) for compounds **5a–e** (Table I) are very similar; the styrene complex **5a** serves as a representative example. Due to the unsymmetrical substitution of the olefin in **5a**, the two pentamethylcyclopentadienyl ligands are inequivalent and appear as two singlets (δ 1.62, 1.47) in the ^{1}H NMR spectrum at 25 °C. The olefinic resonances exhibit typical first-order vinyl patterns as three doublets of doublets. The proton on the phenyl-substituted carbon (H_β) is shifted downfield (δ 2.32, J_{trans} = 13 Hz, J_{cis} = 10 Hz). Assuming the *trans* H–H_β coupling to be larger than the *cis* H–H_β coupling (by analogy to the related styrene oxides), the remaining resonances (δ 0.21 H *cis* to H_β; δ 0.40 H *trans* to H_β, J_{gem} = 6 Hz) can be assigned.

In contrast, the ^{1}H NMR spectrum (90 MHz) of **4** displays a single pentamethylcyclopentadienyl resonance (δ 1.67) at 25 °C due to equilibration of the two inequivalent Cp* ligands via rapid olefin insertion/elimination (vide infra). The ^{1}H NMR for the static structure can be obtained at −40 °C (Table I). Analogous to **5** the two inequivalent pentamethylcyclopentadienyl ligands give rise to singlets (δ 1.60, 1.73) and the hydride resonance (δ −2.95) is broadened by the niobium center ($\nu_{1/2}$ = 6 Hz). At 90 MHz, the vinylic protons appear as complex multiplets.

Attempts to extend the synthesis of $Cp^*_2Nb(olefin)(H)$ complexes to other olefins by reaction **2** were not successful. The reaction of **1** with 1-butene led to olefin isomerization to 2-butene, presumably via metal-mediated hydride–olefin insertion/elimination; however, no metal olefin complex was observed (^{1}H NMR). Attempts to prepare complexes of sterically demanding olefins (neohexene, *o,o*-dimethylstyrene), 1,2-disubstituted olefins (*cis*- and *trans*-2-butene, *cis*- and *trans*-β-methyl styrene), or 1,1-disubstituted olefins (isobutene, *exo*-methylenecyclohexene, α-methylstyrene, diphenylethylene) resulted in intractable oils. Synthesis of heteroatom-substituted ethylene and styrene complexes was also attempted. Acrylonitrile and *p*-chlorostyrene were rapidly polymerized in the presence of **1** or **2**. Vinyl fluoride was transformed to ethylene by reaction with **1**, presumably accompanied by the formation of niobium fluoride derivatives. The products of reaction of **1** with *p*-cyanostyrene and methyl- and ethyl vinyl ethers have not been fully characterized.

In an attempt to assess the relative hydridic or protic nature of the niobium–hydride bond in $Cp^*_2Nb(olefin)(H)$, the reactions of **2** and **5a** with acetone and methanol were examined.[18] In no case was a clean reaction observed,[18c] so that it is not possible to assess the hydridic character of Nb–H in the olefin complex in this manner.

Ligand-Promoted Olefin Insertion to Niobium Alkyls. The reaction of **2** with carbon monoxide (3 atm) at 25 °C results in the slow formation of the insertion product $Cp^*_2Nb(CH_2CH_3)(CO)$ (**6**) (eq 6). Compound **6** is isolated in good yield

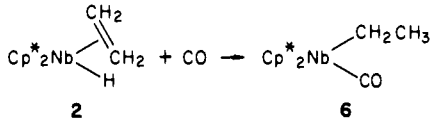

(86%) as a blue-green solid with ν(CO) = 1857 cm^{-1}. The product arising from overall substitution of CO for ethylene, $Cp^*_2Nb(H)(CO)$ (**7**),[14] was also observed in reaction **6** (^{1}H NMR) in up to 20% yields depending on the reaction conditions; performing the reaction in the absence of light reduced the amount of this species to <2%.

Similarly, the styrene derivative **5a** reacts slowly with CO to form the phenethyl carbonyl complex $Cp^*_2Nb(CH_2CH_2Ph)(CO)$ (**8a**) (eq 7). Compound **8a** is isolated as a green crystalline solid

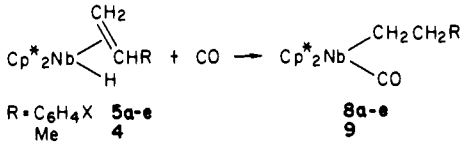

in good yield with ν(CO) = 1867 cm^{-1}. The *para*-substituted styrene complexes **5b–e** form analogous substituted phenethyl derivatives **8b–e** (^{1}H NMR). In contrast to **2** and **5**, **4** reacts with CO immediately in melting benzene-d_6 (0 °C) to form the *n*-propyl derivative **9**. The ^{1}H NMR spectra of **8a** and **8b–e** consist of AA′XX′ patterns for the CH_2CH_2 units consistent with a preferred rotamer (about the C–C bond) having *anti* R(= phenyl or methyl) and niobium substituents.[19]

The niobium olefin hydride complexes **2**, **4**, and **5** react rapidly with a large excess of methyl isocyanide at 25 °C to form alkyl isocyanide derivatives **10** analogous to the CO adducts (eq 8).

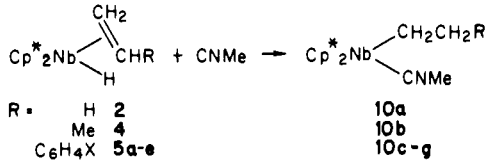

$Cp^*_2Nb(CH_2CH_3)(CNMe)$ (**10a**) and $Cp^*_2Nb(CH_2CH_2Ph)(CNMe)$ (**10c**) are isolated as red crystalline solids in good to moderate yields. **10a** and **10c** exhibit coordinated C≡NMe stretching frequencies in the infrared at 1778 and 1770 cm^{-1}, respectively. These values for ν(C≡NMe) are very low compared to both free CNMe (ν(C≡NMe) = 2163 cm^{-1}) and many other alkyl isocyanide metal derivatives[20] and indicate strong back-

(17) (a) Klazinga, A. H.; Teuben, J. H. *Ibid.* **1980**, *194*, 309–316. (b) Klazinga, A. H. Ph.D. Thesis, University of Groningen, 1979.

(18) (a) Mayer, J. M.; Bercaw, J. E. *J. Am. Chem. Soc.* **1982**, *104*, 2157–2165. (b) Labinger, J. A.; Komadina, K. H. *J. Organomet. Chem.* **1978**, C25–C28. (c) The reaction of $Cp^*_2Nb(olefin)(H)$ with the weak acid MeOH generated H_2, (^{1}H NMR), indicative of a hydridic metal–H bond. Likewise, in the reaction with acetone, an isopropoxy group was observed by ^{1}H NMR, indicating reduction of the ketone by a hydridic hydride. However, in these reactions of $Cp^*_2Nb(olefin)(H)$, olefin dissociation and, for the MeOH addition, hydrogenation were observed, suggesting that these reactions do not assess the hydricity of Nb–H in the olefin complex itself, but in its decomposition products. Nonetheless, this reactivity does appear to support the previously reported hydricity of niobium hydrides.[18b]

(19) Whitesides, G. M.; Witanowski, M.; Roberts, J. D. *J. Am. Chem. Soc.* **1965**, *87*, 2854–2862.

donation into the isocyanide π^* system.[21]

Attempts to trap the olefin insertion product of Cp^*_2Nb(olefin)(H) with other donor ligands (PMe_3, $P(OMe)_3$, $CH_2{=}CH_2$, $MeC{\equiv}N$, tetrahydrofuran, pyridine) were not successful. No reaction was observed to decomposition temperatures except in the case of acetonitrile, for which olefin substitution is observed.[22]

Kinetics of the Insertion of Olefins into Niobium–Hydride Bonds. An indication that reversible olefin insertion and β-H elimination occur for $Cp^*_2Nb(CH_2{=}CHR)(H)$ (eq 9) is obtained by exam-

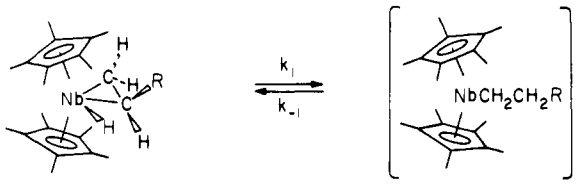

(9)

ination of the variable-temperature ^1H NMR (90 MHz) of **2** (Figure 1). As discussed above, an AA′BB′X pattern is observed at 25 °C (Figure 1) for the two ends of the ethylene ligand and the hydride, which appears as a broad singlet due to coupling to the quadrupolar metal center. As the temperature is raised, the hydride signal and the (δ 0.5) olefin signal broaden and collapse into the base line. Furthermore, on warming, the other olefin signal (δ −0.4) broadens and finally resolves at 90 °C into a multiplet (a pseudo-quartet with $J \cong 7$ Hz). Such changes are consistent with these ethylenic hydrogens experiencing an average coupling ($^2/_3$ (11 Hz) + $^1/_3$ (~0 Hz)) to the other ethylenic hydrogens and the Nb–H. At 160 °C, the weighted average chemical shift of the three exchanging hydrogens appears at δ −0.7. Note that even at this temperature the two ends of the ethylene ligand are not interchanging on the NMR time scale, indicating that olefin rotation is much slower than the insertion and β-H elimination steps. Additionally, the absence of detectable equilibrium amounts of the alkyl tautomer in solutions of the olefin–hydride complexes (^1H NMR) establishes a lower relative limit, $k_{-1} \geqslant 100k_1$, for the rate constant for β-H elimination. Higher temperatures lead to thermal decomposition of **2**.

Due to the complex coupling pattern and the observation of decomposition at temperatures just above coalescence, line-shape analysis from these data was not attempted. Rather, magnetization-transfer experiments[23] (500-MHz ^1H NMR) were undertaken to obtain the forward rate for equilibrium 9. This method does indeed yield the value of k_1. Considerations in the application of this experiment to the $Cp^*_2Nb(CH_2{=}CHR)(H)$ system are discussed in the supplementary material.

Figure 2 shows typical data collected as a series of spectra for magnetization transfer from the (CH_2) group of ethylene to the hydride in **2** at 59 °C. The experiment involves selectively inverting one of the exchanging signals and then waiting a specified time before observing the spectrum. The correlation of the difference in intensity of the peaks due to the exchanging nuclei as a function of delay time according to the magnetization equation[24] yields the exchange rate. For **2** the k_1 process leads to the magnetization transfer on average only two-thirds of the time when the (CH_2) resonance is inverted; therefore, the exchange rate constant[25] is related to the insertion rate constant by $k_{exchange} = (2/3)k_1$. Similar statistical considerations give $k_{exchange} = (1/3)k_1$ for **2** when the hydride resonance is inverted and $k_{exchange} = (1/2)k_1$

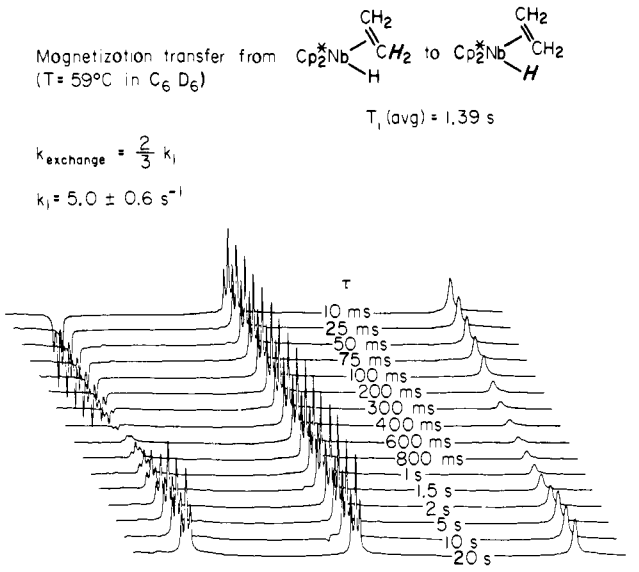

Figure 2. Magnetization transfer experiment for $Cp^*_2Nb(CH_2{=}CH_2)(H)$.

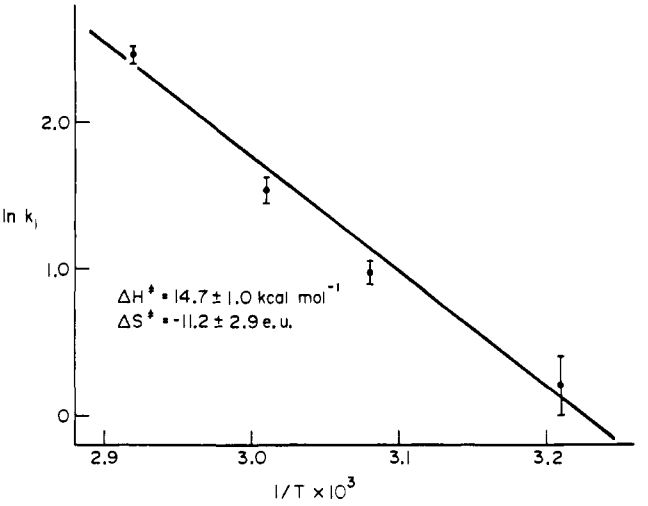

Figure 3. Arrhenius plot for the hydride–olefin insertion reaction for $Cp^*_2Nb(CH_2{=}CH_2)(H)$.

for **5a–e**. The nonlinear least-squares fit[24] of the spectra in Figure 2 to the magnetization equation leads to $k_1 = 5.03$ (61) s^{-1} at 59 °C. The measured rates are equivalent within experimental error whether olefinic or hydridic resonances are inverted (Table II). The rate is invariant over a fourfold concentration range of **2**, indicating that olefin insertion is unimolecular as required by the observed NMR behavior. The intensity for the olefin α(*exo*) hydrogen[26] signals remains constant during the magnetization-transfer experiments. This observation together with the variable-temperature ^1H NMR behavior for **2** (Figure 1) indicates that insertion pathways involving the α hydrogens are not important.[27]

(20) Treichel, P. M. *Adv. Organomet. Chem.* **1973**, *11*, 21–86 and references therein.

(21) Klazinga, A. H.; Teuben, J. H. *J. Organomet. Chem.* **1980**, *192*, 75–81.

(22) Doherty, N. M. Ph.D. Thesis, California Institute of Technology, 1984.

(23) Sandström, J. "Dynamic NMR Spectroscopy"; Academic Press: London, England, 1982.

(24) (a) Perkin, T. Ph.D. Thesis, California Institute of Technology, 1981 and references therein. (b) Supplementary material.

(25) For inversion of the (CH_2) resonance of **2**, the analysis used (ref 24) yields $k_{exchange}$ from the hydride site which equals $(2/3)k_1$. Similarly, for **2** when the hydride resonance is inverted $k_{exchange}$ from the (CH_2) site (=$(1/3)k_1$) is determined.

(26) (a) For the discussion of the hydride–olefin insertion process, the following labeling scheme is employed. In the alkyl tautomer, [$Cp^*_2NbCH_2CH_2R$], the carbon bound to the metal is labeled α; the carbon bearing the R substituent, β (consistent with the idea of β-H elimination from this carbon). The carbons and hydrogens in the olefin hydride complex, $Cp^*_2Nb(CH_2{=}CHR)(H)$, are consequently labeled corresponding to the alkyl tautomer: the *exo* carbon and its hydrogens are labeled α; the *endo* carbon and its hydrogen(s), β.

(27) Pathways including alkylidene $Cp^*_2Nb({=}CHCH_2R)(H)$ and vinyl $Cp^*_2Nb(CH{=}CHR)(H)_2$ intermediates, "dyotropic rearrangement" (ref 28 and 29) of $Cp_2NbCH_2CH_2H$ to $HCH_2CH_2NbCp^*_2$, or any other process which involves the α hydrogens in the exchange process, including olefin rotation, can be ruled out on the NMR time scale based on the observed dynamic NMR behavior. It is possible, however, that processes such as these are important on the chemical time scale, for example, in the observed scrambling of protons into the α hydrogen positions in the synthesis of 2-d_m.

Table I. NMR[a] and IR[b] Data

compd	IR	NMR (chemical shift, multiplicity, coupling Constants) assignment	^{1}H	^{13}C
$Cp^*_2Nb(CH_2{=}CH_2)(H)$ (**2**)[c,d]	ν(Nb–H) 1710	$C_5(CH_3)_5$	1.63 s	11.3 q, J = 126
	ν(Nb–D) 1238	$C_5(CH_3)_5$		102.9 s
		$CH_2{=}CH_2'$	−0.23 t, J = 11	20.8 t, J = 147
		$CH_2{=}CH_2'$	0.65 td, J = 11, 2	25.5 td, J = 150, 6
		Nb—H	−3.04 s	
$Cp^*_2Nb(CH_2{=}CHMe)(H)$ (**4**)[e]	ν(Nb–H) 1718	$C_5(CH_3)_5$	1.60 s	11.7 q, J = 126
			1.73 s	
		$C_5(CH_3)_5$		104.2 s
		$CH_2{=}CHCH_3$	0.08 m ABX	29.8 t, J = 146
		$CH_2{=}CHCH_3$	0.90 m	37.8 d, J = 138
		$CH_2{=}CHCH_3$	2.26 d, J = 7	25.1 q, J = 123
		Nb—H	−2.95 s	
$Cp^*_2Nb(CH_2{=}CHPh)(H)$ (**5a**)[c]	ν(Nb–H) 1743, 1679[f]	$C_5(CH_3)_5$	1.47 s	11.1 q, J = 127
		$C_5(CH_3)_5'$	1.62 s	11.4 q, J = 127
		$C_5(CH_3)_5$		104.8 s
		$C_5(CH_3)_5'$		105.4 s
		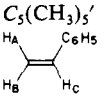	0.40 dd, J_{AB} = 6	
			0.21 dd, J_{BC} = 11	
			2.32 dd, J_{AC} = 13	
		Nb—H	−2.24 s	
		$CHH'{=}CHC_6H_5$		24.0 dd, J = 147, 145
		$CHH'{=}CHC_6H_5$		45.8 d, J = 142
		$CHH'{=}CHC_6H_5$	6.97 t, J = 7	123.3 dt, J = 152, 7
			7.25 t, J = 7	127.5 dd, J = 156, 7
			7.72 d, J = 7	130.3 d, J = 160
				151.6 s
$Cp^*_2Nb(CH_2{=}CHC_6H_4\text{-}p\text{-}NMe_2)(H)$ (**5b**)[c]	ν(Nb–H) 1769, 1712[f]	$C_5(CH_3)_5$	1.53 s	11.2 q, J = 126
		$C_5(CH_3)_5'$	1.66 s	11.5 q, J = 126
		$C_5(CH_3)_5$		104.5 s
		$C_5(CH_3)_5'$		105.0 s
		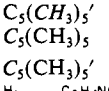	0.45 dd, J_{AB} = 6	
			0.26 dd, J_{BC} = 11	
			2.37 dd, J_{AC} = 13	
		$N(CH_3)_2$	2.65 s	41.4 q, J = 132
		Nb—H	−2.27 s	
		$CHH'{=}CHC_6H_4N(CH_3)_2$		24.5 t, J = 145
		$CHH'{=}CHC_6H_4N(CH_3)_2$		45.8 d, J = 144
		$CHH'{=}CHC_6H_4N(CH_3)_2$	6.78 d, J = 8	112.9 d, J = 152
			7.72 d, J = 8	131.2 dd, J = 154, 7
				139.6 s
				147.6 s
$Cp^*_2Nb(CH_2{=}CHC_6H_4\text{-}p\text{-}OMe)(H)$ (**5c**)[c]	ν(Nb–H) 1745[g]	$C_5(CH_3)_5$	1.50 s	11.2 q, J = 126
		$C_5(CH_3)_5'$	1.63 s	11.5 q, J = 125
		$C_5(CH_3)_5$		104.7 s
		$C_5(CH_3)_5'$		105.2 s
		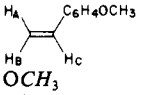	0.37 dd, J_{AB} = 5	
			0.22 dd, J_{BC} = 10	
			2.29 dd, J_{AC} = 14	
		OCH_3	3.44 s	44.9 q, J = 143
		Nb—H	−2.30	
		$CHH'{=}CHC_6H_4OCH_3$		24.5 t, J = 146
		$CHH'{=}CHC_6H_4OCH_3$		45.5 d, J = 143
		$CH_2{=}CHC_6H_4OCH_3$	6.89 d, J = 8	112.9 dd, J = 157, 5
			7.67 d, J = 7	131.2 dd, J = 168, 6
				143.1 s
				156.2 s
$Cp^*_2Nb(CH_2{=}CHC_6H_4\text{-}p\text{-}Me)(H)$ (**5d**)[c]	ν(Nb–H) 1738[g]	$C_5(CH_3)_5$	1.50 s	11.1 q, J = 127
		$C_5(CH_3)_5'$	1.63 s	11.5 q, J = 127
		$C_5(CH_3)_5$		104.7 s
		$C_5(CH_3)_5'$		105.3 s
		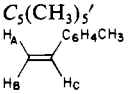	0.41 dd, J_{AB} = 5	
			0.22 dd, J_{AC} = 10	
			2.32 dd, J_{AC} = 14	
		$C_6H_4CH_3$	2.28 s	21.2[h]
		Nb—H	−2.25 s	
		$CHH'{=}CHC_6H_4CH_3$		24.1 t, J = 142
		$CHH'{=}CHC_6H_4CH_3$		45.7 d, J = 145
		$CHH'{=}CHC_6H_4CH_3$	7.10 d, J = 6	130.4 d, J = 158
			7.68 d, J = 6	131.1[h]

Table I (Continued)

compd	IR	NMR (chemical shift, multiplicity, coupling Constants) assignment	^{1}H	^{13}C
				148.1 d, J = 10
$Cp^*_2Nb(CH_2{=}CHC_6H_4\text{-}p\text{-}CF_3)(H)$ (**5e**)[c]	ν(Nb–H) 1737, 1692	$C_5(CH_3)_5$	1.39 s	11.0 q, J = 127
		$C_5(CH_3)_5'$	1.57 s	11.4 q, J = 126
		$C_5(CH_3)_5$		105.1 s
		$C_5(CH_3)_5'$		105.8 s
		H_A, $C_6H_4CF_3$, H_B, H_C	0.29 dd, J_{AB} = 6	
			0.16 dd, J_{BC} = 10	
			2.16 dd, J_{AC} = 13	
		CF_3	^{19}F NMR 102.5 s[i]	54.6[h]
		Nb—H	−2.27 s	
		$CHH'{=}CHC_6H_4CF_3$		23.9 t, J = 146
		$CHH'{=}CHC_6H_4CF_3$		44.8 d, J = 140
		$CHH'{=}CHC_6H_4CF_3$	7.46	124.2 d, J = 158
			7.52	124.4 d, J = 158
				130.1 s
				157.4 s
$Cp^*_2Nb(Et)(CO)$ (**6**)	ν(CO) 1857[g]	$C_5(CH_3)_5$	1.62 s	10.7 q, J = 127
		$C_5(CH_3)_5$		101.9 s
		$NbCH_2CH_3$	−0.03 q, J = 8	(not found)
		$NbCH_2CH_3$	1.61 t, J = 8	22.8 q, J = 122
		NbCO		280.2 s, $\nu_{1/2}$ = 88 Hz[j]
$Cp^*_2Nb(CH_2CH_2Ph)(CO)$ (**8a**)	ν(CO) 1867[g]	$C_5(CH_3)_5$	1.58 s	10.7 q, J = 127
		$C_5(CH_3)_5$		102.0 s
		$NbCH_2CH_2C_6H_5$	0.02 m AA′XX′	20.1 t, J = 120
		$NbCH_2CH_2C_6H_5$	2.84 m	46.1 t, J = 125
		$NbCH_2CH_2C_6H_5$	7.15–7.66	124.7 dt, J = 160, 7
				128.4 d, J = 158
				151.9 s
		NbCO		280.1 s, $\nu_{1/2}$ = 66 Hz[j]
$Cp^*_2Nb(Et)(CNMe)$ (**10a**)	ν(C≡NMe) 1778	$C_5(CH_3)_5$	1.70 s	11.1 q, J = 126
		$C_5(CH_3)_5$		104.2 s
		$NbCH_2CH_3$	0.04 q, J = 7	23.6 t, J = 122
		$NbCH_2CH_3$	1.71 t, J = 7	11.9 q, J = 127
		$CNCH_3$	3.23 s	37.5 q, J = 138
		$CNCH_3$		209.5 s
$Cp^*_2Nb(CH_2CH_2Ph)(CNMe)$ (**10c**)	ν(C≡NMe) 1770	$C_5(CH_3)_5$	1.67 s	11.1 q, J = 126
		$C_5(CH_3)_5$		104.2 s
		$NbCH_2CH_2C_6H_5$	0.14 m AA′XX′	24.5 t, J = 125
		$NbCH_2CH_2C_6H_5$	2.94 m	50.0 q, J = 126
		$NbCH_2CH_2C_6H_5$	7.24–7.55 m	124.7 d, J = 158
				128.4 d, J = 157
				151.9 s
		$CNCH_3$	3.23 s	37.6 q, J = 138
		$CNCH_3$		(not found)

[a] ^{1}H (90 MHz) and ^{13}C (22.5 MHz) NMR spectra taken in benzene-d_6 at ambient temperature unless otherwise noted. Chemical shifts are reported in δ relative to internal Me_4Si or residual protons or carbons in solvent. Coupling constants are reported in Hz. Long-range ^{13}C–^{1}H coupling is reported only when a coupling constant could be determined. [b] IR spectra obtained as Nujol mulls except where indicated. Values given in cm^{-1}. The complete spectra are detailed in the Experimental Section. [c] ^{1}H NMR spectrum obtained at 500 MHz. [d] ^{13}C NMR spectrum obtained at 125 MHz. [e] ^{1}H NMR spectrum obtained in toluene-d_8 at −40 °C. [f] Two bands of similar intensity are observed in the metal hydride stretching region. It has not been possible to assign ν(Nb–H) definitely. [g] IR spectrum obtained for C_6D_6 solution. [h] Chemical shift determined from proton-decoupled spectrum. Coupling constant could not be determined due to overlapping resonances or insufficient signal-to-noise in gated spectrum. [i] ^{19}F NMR (84 MHz) obtained in benzene-d_6 relative to C_6F_6 external standard at δ = 0. [j] Chemical shift value obtained from ^{13}C(^{1}H) NMR of sample prepared from ^{13}CO in the presence of excess ^{13}CO. Extreme broadening of the ^{13}CO NMR signals is presumed to be due to coupling to the quadrupolar Nb nucleus since a sharp singlet was observed for the free ^{13}CO in solution.

Exchange rates, measured for **2** and **5a–e**, the k_1 values determined from these experiments, and the data used to calculate these values are given in Table II. Arrhenius plots for **2** and **5a** yield activation parameters as shown in Figures 3 and 4.

It is possible to obtain an independent check on the activation parameters obtained from the magnetization-transfer experiment by examining the coalescence of the pentamethylcyclopentadienyl resonances of **5a**. A check was deemed useful since magnetization transfer had not previously been applied to a system involving exchanging protons which are coupled to nonexchanging protons. Conveniently, the (η^5-C_5Me_5) resonances of the styrene complexes are inequivalent (^{1}H NMR). Insertion to form the phenethyl tautomer followed by rapid rotation about the $NbCH_2$–CH_2Ph bond and fast β-H elimination may effect site exchange for the two pentamethylcyclopentadienyl groups as shown in Scheme I. At 83 °C the two resonances due to the (η^5-C_5Me_5) ligands of **5a** do indeed coalesce. Complete line-shape analysis of this equally

Scheme I

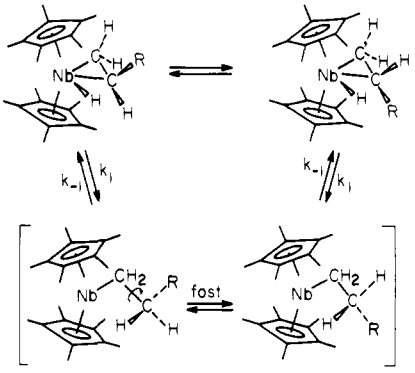

populated AX system was not performed; however, a good value for k_1 may be obtained at the coalescence temperature.[23] The k_1 value measured (Table III) in this way fits satisfactorily on the Arrhenius plot for **5a** (Figure 4).

(28) Reetz, M. T. *Adv. Organomet. Chem.* **1977**, *16*, 33.
(29) Erker, G. *Acc. Chem. Res.* **1984**, *17*, 103–109.

Table II. Exchange and Insertion Rates for Reversible Olefin Insertion/Elimination for **2** and **5a–e** (eq 9) Obtained by Magnetization Transfer Experiments (Benzene-d_6)

compd	T, °C	resonance inverted	T_1,[a] s	k_{ex}, s^{-1}	k_1, s^{-1}
2	39	$CH_2{=}CH_2$	1.01	0.82 (36)	1.24 (24)
	39	Nb—*H*	1.17	*b*	*b*
	52	$CH_2{=}CH_2$	1.69	1.98 (17)	2.97 (26)
	52	Nb—*H*	1.71	0.80 (10)	2.41 (29)
	59	$CH_2{=}CH_2$	1.39	3.35 (41)	5.03 (61)
	59	Nb—*H*	1.40	1.50 (16)	4.49 (49)
	70	$CH_2{=}CH_2$	1.58	7.26 (80)	10.9 (12)
	70	Nb—*H*	1.65	4.30 (28)	12.9 (8)
5a	48	$CH_2{=}CHR$	1.22	1.40 (12)	2.81 (24)
	48	Nb—*H*	0.93	1.15 (10)	2.31 (19)
	59	$CH_2{=}CHR$	1.08	2.89 (28)	5.79 (56)
	59	Nb—*H*	1.09	2.96 (22)	5.92 (43)
	70	$CH_2{=}CHR$	1.28	10.6 (6)	21.1 (12)
	70	Nb—*H*	1.34	10.9 (6)	21.7 (12)
5b	50	$CH_2{=}CHR$	0.83	3.44 (55)	6.88 (109)
	50	Nb—*H*	0.75	3.36 (28)	6.72 (56)
5c	48	$CH_2{=}CHR$	0.71	1.91 (29)	3.82 (58)
	48	Nb—*H*	0.72	2.21 (18)	4.43 (36)
5d	49	$CH_2{=}CHR$	1.06	*c*	*c*
	49	Nb—*H*	0.82	1.60 (35)	3.19 (69)
5e	76	$CH_2{=}CHR$	1.28	2.07 (21)	4.14 (43)
	76	Nb—*H*	1.06	2.55 (20)	5.09 (40)

[a] Longitudinal relaxation times (T_1) for proton(s) listed as inverted resonance obtained by normal inversion–recovery method. [b] A good value for k_{ex} (and, hence, k_1) could not be obtained in this experiment due to its small value under these conditions. [c] A good value for k_{ex} (and k_1) could not be obtained by this experiment due to overlap of the $CH_2{=}CHR$ and p-CH_3 signals in the ^{1}H NMR.

Table III. Olefin Insertion Rates for **4** and **5a–e** (eq 9) Obtained by the Coalescence Method (Scheme I)

compd	$\Delta\nu$, Hz	coalescence T, °C	$k_{coalescence}$ k_1, s^{-1}	$\Delta G^{\ddagger}$, kcal mol^{-1}
4	11.4 (5)[a]	−1 (1)	25.3 (11)	14.1 (1)
5a	13.3 (6)[b]	83 (1)	29.5 (13)	18.6 (1)
5b	11.2 (5)[b]	69 (1)	24.9 (11)	17.9 (1)
5c	12.5 (5)[b]	75 (1)	27.8 (11)	18.2 (1)
5d	12.0 (6)[b]	77 (1)	26.7 (13)	18.3 (1)
5e	16.2 (6)[b]	115 (1)	36.0 (13)	20.2 (1)

[a] Measured at −40 °C. [b] Measured at 25 °C.

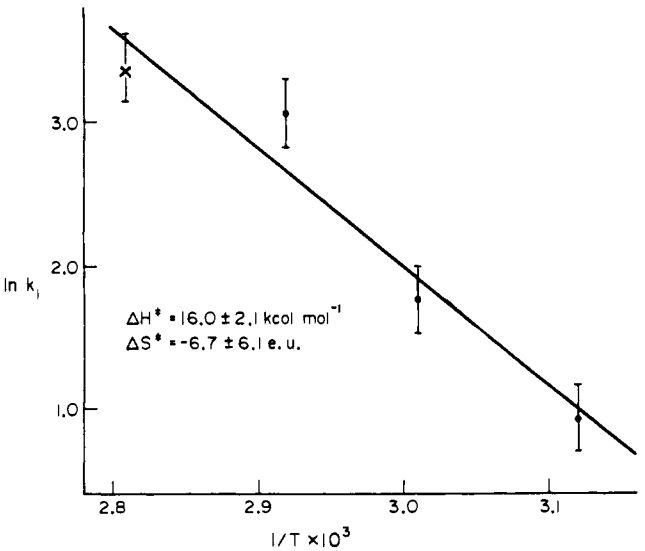

Figure 4. Arrhenius plot for the hydride–olefin insertion reaction of $Cp^*_2Nb(CH_2{=}CHPh)(H)$. ● = magnetization transfer data; × = coalescence data.

Use of the coalescence method allowed rapid determination of k_1 for **5b–e** at a second temperature, thus allowing approximate determination of the temperature dependence of k_1 for these compounds. The k_1 for insertion of propene into the niobium–hydride bond of **4** was also measured by this method. The k_1 values at coalescence for **4** and **5a–e** are given in Table III. The temperature-dependent variables for the k_1 values for **2** and **5a–e**, as calculated by the Arrhenius equation, are given in Table IV. The insertion rates for **2**, **4**, and **5a–e** at 50 °C are calculated from these data and given in Table V. Hammett plots[30] for the styrene

Table IV. Arrhenius Parameters for the Hydride–Olefin Insertion Reaction for **2** and **5a–e**

R	log A	E_a, kcal mol^{-1}	$\Delta S^{\ddagger}$, eu	$\Delta H^{\ddagger}$, kcal mol^{-1}
H	10.8	15.3 (1.0)	−11.2 (2.9)	14.7 (1.0)
Ph	11.8	16.7 (2.1)	−6.7 (6.1)	16.0 (2.1)
p-$Me_2NC_6H_4$	10.5	14.3 (1.0)	−12.5 (2.9)	13.7 (1.0)
p-$MeOC_6H_4$	11.0	15.2 (0.7)	−10.6 (2.0)	14.5 (0.7)
p-MeC_6H_4	12.0	16.9 (2.0)	−5.8 (5.7)	16.2 (2.0)
p-$CF_3C_6H_4$	9.5	14.1 (0.5)	−17.2 (1.4)	13.4 (0.5)

Table V. Rates for Olefin Insertion into the Niobium–Hydride Bonds of $Cp^*_2Nb(CH_2{=}CHR)(H)$ (50 °C, Benzene-d_6)

R	k_1,[a] s^{-1}	$\Delta G^{\ddagger}$, kcal mol^{-1}
H	2.62 (16)	18.3 (1)
Me	890 (320)[b]	14.6 (2)[b]
Ph	3.18 (58)	18.2 (1)
p-Me_2N–C_6H_4	6.80 (50)	17.7 (1)
p-MeO–C_6H_4	4.81 (35)	17.9 (1)
p-Me–C_6H_4	3.47 (81)	18.1 (2)
p-CF_3–C_6H_4	0.91 (11)	19.0 (1)

[a] Measured at, interpolated to, or extrapolated to 50 °C. [b] Extrapolated from k_1 and $\Delta G^{\ddagger}$ measured by the coalescence experiment at −1 °C assuming $\Delta S^{\ddagger} = -10 \pm 4$ eu.

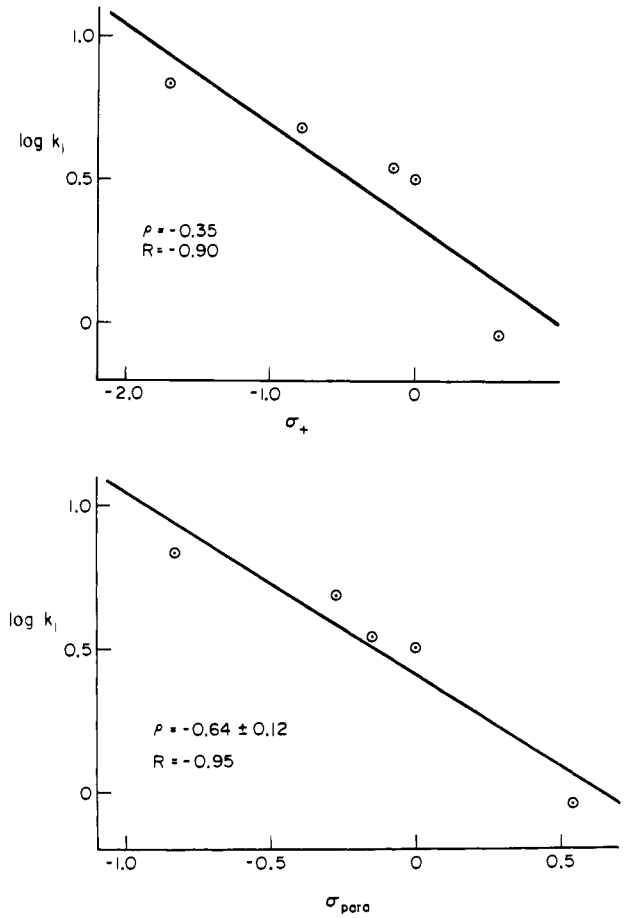

Figure 5. Hammett plots for the para substituent effects on the rate of hydride–olefin insertion at 50 °C.

(30) Values of σ and σ^+ were taken from ref 43 except for σ^+ for CF_3 which is from Swain, M. S. *J. Am. Chem. Soc.* **1983**, *105*, 492–502.

Scheme II

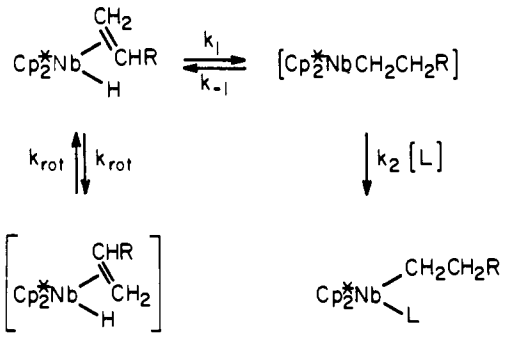

Table VI. Solvent Effects on the Hydride–Olefin Insertion Barrier for **5a**

solvent	ϵ^a	$\Delta\nu$, 25 °C, Hz	coalescence T, °C	$\Delta G^{\ddagger}$, kcal mol^{-1}
benzene-d_6	2.28	13.3 (6)	83 (1)	18.6 (1)
tetrahydrofuran-d_8	7.32	23.3 (10)	91 (1)	18.6 (1)
pyridine-d_5	12.3	16.5 (10)	90 (1)	18.8 (1)
dimethylformamide-d_7	36.7	22.8 (10)	92 (2)	18.7 (2)

^{a} Dielectric constant for pure protio solvent at 25 °C.

complexes **5a–e** are shown in Figure 5. The data correlate better with σ than σ^+, as shown with $\rho = -0.64$.

Measurement of the insertion rate during chemical trapping experiments was also attempted. As discussed previously, CO and CNMe trap the unsaturated intermediate [$Cp^*_2Nb(CH_2CH_2R)$] to give alkyl derivatives (Scheme II). Scheme II leads to the rate expression shown in eq 10. In principle, it should be possible

$$-\frac{d[A]}{dt} = k_{obsd}[A] = \frac{k_1k_2[L]}{k_{-1} + k_2[L]}[A] \qquad (10)$$

to determine k_1 from the dependence of k_{obsd} on the [L], provided a regime can be found in which less than first-order dependence on [L] is observed.[31] The reaction of **2** with varying concentrations of CNMe in benzene-d_6 was monitored at 46 °C (eq 8).

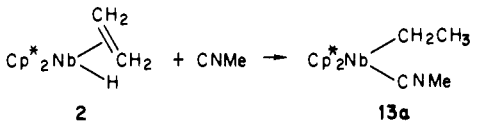

The reaction kinetics, as measured by loss of **2** vs. time (^{1}H NMR), were first order in **2**. The overall rate shows a first-order dependence on the [CNMe]. It is concluded that the kinetics of reaction 8 (Scheme II) are best described by a rapid preequilibrium insertion/β-H elimination followed by slow, rate-limiting bimolecular trapping. Consequently, in this temperature and concentration regime, it is not possible to obtain k_1 from ligand-trapping kinetics.

As mentioned previously, pyridine and tetrahydrofuran do not promote olefin insertion to form solvated alkyl derivatives, $Cp^*_2Nb(CH_2CH_2R)(S)$. Nonetheless, the possibility still exists that good ligating solvents could accelerate the insertion process without effecting an observable shift in equilibrium, as has been observed for the migratory insertion of alkyl carbonyl complexes.[32] Since **5a** is moderately stable in THF-d_8, pyridine-d_5, and DMF-d_7 at elevated temperatures, the insertion barrier in these solvents was determined by the coalescence technique. The data (Table VI) show no significant variation in $\Delta G^{\ddagger}$ for **5a** among the four solvents, thus negating the possibility of solvent-promoted insertion. Moreover, it may be concluded that there is no substantial difference in solvation of ground and transition state.

(31) For strict first-order dependence of the rate on [L], eq 10 becomes $k_{obsd}[A] = (k_1k_2[L]/k_{-1})[A]$ and $1/k_{obsd}$ vs. $1/[L]$ should have a zero-intercept, as is observed for reaction **9** within experimental error.

(32) Wax, M. J.; Bergman, R. G. *J. Am. Chem. Soc.* **1981**, *103*, 7028–7030.

Table VII. Equilibrium Data for Competitive Binding of Ethylene, Propene and Styrene (Eq 11) (25 °C, Benzene-d_6)

R	K_{eq}	$\Delta G°$, kcal mol^{-1}
H	1	0
Me	0.0069 (17)	2.9 (2)
Ph	0.047 (4)	1.8 (1)
p-Me_2N–C_6H_4	0.032 (3)	2.0 (1)
p-MeO–C_6H_4	0.041 (3)	1.9 (1)
p-Me–C_6H_4	0.039 (4)	1.9 (1)
p-CF_3–C_6H_4	0.040 (3)	1.9 (1)

Table VIII. Free Energy Data for Olefins (25 °C, Gas)[a]

R	$\Delta G°_f$ (CH_2=CHR)	$\Delta G°_f$ (CH_3CH_2R)	$\Delta G°_{hydrog}$	$\Delta(\Delta G°_{hydrog})$[b]
H	16.282	−7.860	−24.142	0
Me	14.990	−5.614	−20.604	−3.54
Ph	51.10	31.208	−19.892	−4.25
p-MeC_6H_4	50.24	30.281	−19.959	−4.18

^{a} From ref 34. Values are given in kcal mol^{-1}. ^{b} Relative to ethylene.

Table IX. Relative Binding Energies for Ethylene, Propene, and Styrene Complexes, $Cp^*_2Nb(CH_2$=CHR)(H) (**2**, **4**, **5a**, **6d**)

R	$\Delta G°$ (eq 12)	$0.5\Delta(\Delta G°_{hydrog})$	rel G.S. E. for olefin complex[a]
H	0	0	0
Me	2.9 (2)	−1.8	1.1
Ph	1.8 (1)	−2.1	−0.3
p-MeC_6H_4	1.9 (1)	−2.1	−0.2

^{a} Relative ground state energy for olefin complex.

To assess the ground-state effects of olefin coordination on the insertion barrier, competitive binding of the substituted olefin to the metal center relative to ethylene (eq 12) was examined. The

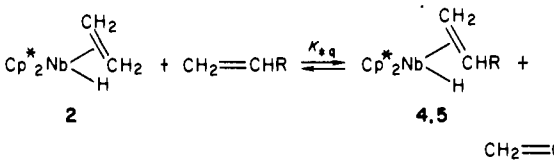

CH_2=CH_2 (12)

equilibrium concentrations (^{1}H NMR) were approached from both sides of eq 12 and converged to a single value in each case. Equilibrium constants (Table VII) were measured only at 25 °C because at elevated temperatures significant polymerization was observed.

In order to place the ground states and insertion transition states for the different olefin hydride complexes on a common energy surface, the contributions of the free olefins in equilibrium 12 must be taken into account; that is, one would like to know the relative energies of $Cp^*_2Nb(CH_2$=$CH_2)(H)$ and $Cp^*_2Nb(CH_2$=CHR)(H) in the absence of the uncoordinated olefins. Coordination of an olefin to the niobium center involves a partial reduction of the double bond, suggesting olefin hydrogenation (reduction of the olefin double bond by H_2) as a model for this process. According to this model, an olefin which is hydrogenated more exothermically than another has a less stable double bond with respect to the coordination equilibrium (eq 12). Thus, comparison of the free energies of hydrogenation for the olefins CH_2=CH_2 and CH_2=CHR provides a quantitative measure of their relative free energies (free olefin vs. olefin coordinated to niobium).[33]

(33) This analysis relies on the assumptions that binding of any olefin, CH_2=CHR, to the fragment [Cp^*_2NbH] can be described by separate energetic contributions due to the olefin double bond and to olefin coordination and that olefin hydrogenation provides a reasonable model for the relative double bond energies. A referee has suggested that the free energies of solvation of the olefins be used either to correct the gas-phase free energies of hydrogenation or in place of the free energies of hydrogenation in the assessment of the contribution of uncoordinated olefins to equilibrium 12. Solvation of all species in equilibrium 12 is, of course, included in the measured equilibrium data, but, we do not see a straightforward way to assess these effects on the difference in ground states energies for $Cp^*_2Nb(CH_2$=$CH_2)(H)$ $Cp^*_2Nb(CH_2$=CHR)(H).

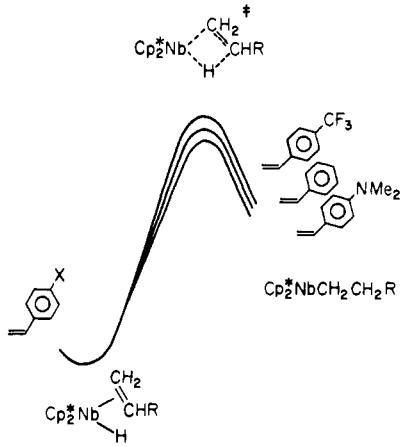

Figure 6. Partial free-energy surfaces for insertion of styrenes into the niobium–hydride bond.

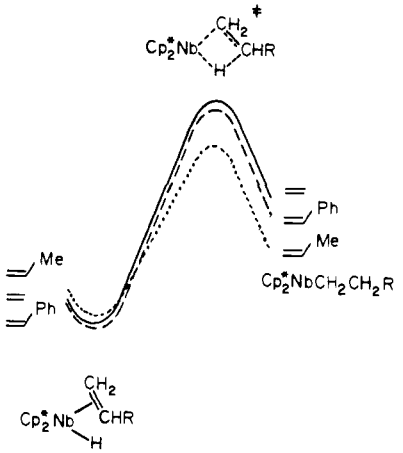

Figure 7. Partial free-energy surfaces for insertion of ethylene, propene, and styrene into the niobium–hydride bond.

The values of ΔG°_{hydro}, calculated from the difference in free energies of formation for the olefin and its corresponding saturated hydrocarbons[34] are shown in Table VIII. As can be seen from these data, ethylene has a more readily reduced double bond than propene, styrene, or *p*-methylstyrene. Consequently, the position of equilibrium 12, which favors the ethylene complex **2** in all cases, is due, in part, to the fact that free ethylene has a less stable double bond than the other free, substituted olefins. A fraction (0.5) of the difference in the free energies of hydrogenation of substituted olefins and ethylene was used to adjust ΔG° as shown in Table IX. The very approximate factor of 0.5 is used since ^{1}H and ^{13}C NMR data for the ethylene ligand of **2** suggest that the C–C bond order of ethylene coordinated to niobium is approximately 1.5.[35] The relative energies calculated in this manner were used to order the ground states of the various olefin hydride complexes in Figure 7.

Kinetic and Thermodynamic Isotope Effects for the Insertion of Ethylene into the Niobium–Hydride Bond. Preparation of deuterium-substituted niobium olefin hydride complexes is not straightforward. The reaction of **1** or $Cp^*_2NbD_3$ (**1**-d_3)[22] with ethylene-d_4 at 100 °C results in significant incorporation of deuterium into the cyclopentadienyl methyl groups and approximately one proton averaged among the five ethylene and hydride sites (^{1}H and ^{2}H NMR). Nonetheless, this partially deuterated ethylene complex, $(Cp^*\text{-}d_n)_2Nb(CX_2{=}CX_2)(X)$ (**2**-d_m; X = H or D), does allow evaluation of the thermodynamic isotope effect for this system. Assuming that at 25 °C exchange of only the endo (β) protons of the olefin in 2-d_m with the hydride is occurring, due to rapid reversible hydride–olefin insertion, the ratio of proton to deuterium (^{1}H and ^{2}H NMR) in the two exchanging positions will reflect the thermodynamically preferred arrangement of hydrogen isotopes in these sites due to their zero-point energy differences. **2**-d_m can be described as a mixture of $(Cp^*\text{-}d_n)_2Nb(CX_2{=}CD_2)(D)$ (A), $(Cp^*\text{-}d_n)_2Nb(CX_2{=}CD_2)(H)$ (B), and $(Cp^*\text{-}d_n)_2Nb(CX_2{=}CDH)(D)$ (C) with B and C related by reversible olefin insertion (eq 13). Consideration of the equilibrium fractional concentrations (25 °C, benzene) of B (0.35 ± 0.05) and C (0.38 ± 0.06) by ^{1}H NMR spectroscopy and the different populations of the two exchanging sites leads to a thermodynamic isotope effect (C/2B) = 0.55 ± 0.09 or ΔE = 0.35 ± 0.11 kcal/mol^{-1} for eq 13.[36] As expected, the lighter isotope (H) prefers the site of lower vibrational energy (Nb–H bond), the heavier isotope (D), the site of higher vibrational energy (C–D bond).

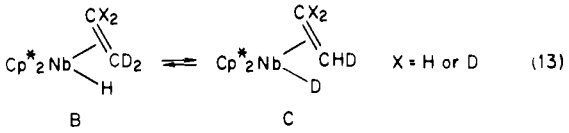

In contrast to the thermal reaction of **1** with ethylene-d_4, $[(C_5(CH_3)_5]_2Nb(CD_2{=}CD_2)(D)$ (**2**-d_5) is cleanly prepared by the reaction of **3** with (ethyl-d_5) magnesium bromide at 25 °C. The rate of insertion of ethylene-d_4 into the Nb–D bond of **2**-d_5 (eq 14) was measured by the coalescence method using ^{2}H NMR.

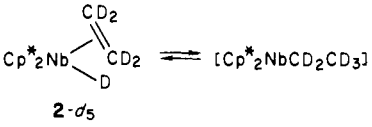

The *endo* (β) deuterons (δ 0.48, 2 D) and the deuteride (δ −3.16, 1 D) appear as broad singlets in the proton-decoupled deuterium NMR. Coalescence of the two unequally populated signals occurs at 105 ± 5 °C. Using the method described by Shanan-Atidi and Bar-Eli,[37] the rate of exchange for this 2:1 population system with $\Delta\nu$ = 50.0 ± 0.5 Hz is calculated to be k_1 = 76 ± 2 s^{-1} at coalescence.[38a] From the Eyring equation, $\Delta G^\ddagger$ (105 °C) = 19.0 ± 0.3 kcal mol^{-1} is obtained. Using the observed temperature dependence of the insertion rate for **2**, the rate of insertion for the protio system can be extrapolated to 105 °C:[38b] k_1 = 84 ± 22 s^{-1}. From these data a kinetic deuterium isotope effect k_H/k_D = 1.1 ± 0.4 is calculated.

Discussion

A series of compounds which allows a systematic study of the insertion of olefins into metal–hydride bonds has been examined. The rate constant k_1, which is directly measurable by dynamic NMR techniques, reflects the barrier to olefin insertion for the niobium complexes (eq 9). The relative ground-state energies for

(34) (a) ΔG_f° (gas, 25 °C) values from "CRC Handbook of Chemistry and Physics", 59th ed., pp D82–D84, except for ΔG_f° for p-$MeC_6H_4CH_2CH_3$ which was obtained from "Selected Values of Physical and Thermodynamic Properties of Hydrocarbons and Related Compounds"; American Petroleum Institute, Project 44, Carnegie Institute of Technology: Pittsburgh, PA, 1953. (b) ΔG_f° (25 °C, gas) for H_2 = 0 kcal mol^{-1}.

(35) ^{1}H and ^{13}C NMR data for the ethylene ligand of **2** are very similar to those for $Cp^*_2Ti(CH_2{=}CH_2)$, the structural features of which indicate the metal–olefin bonding as halfway between a dative olefin-to-metal interaction and a metallocyclopropane.[14b] (See Note Added in Proof.)

(36) Although three other isomers, $(Cp^*\text{-}d_n)_2Nb(CX_2{=}CDH)(H)$, $(Cp^*\text{-}d_n)_2Nb(CX_2{=}CH_2)(D)$, and $(Cp^*\text{-}d_n)_2Nb(CX_2{=}CH_2)(H)$, are also present, their amounts are statistically very small; only approximately one proton is distributed among the five ethylene and hydride sites (^{1}H and ^{2}H NMR). (See Experimental Section.)

(37) Shanan-Atidi, H.; Bar-Eli, K. H. *J. Phys. Chem.* **1970**, *74*, 961–963.

(38) (a) Although the β deuteron and deuteride signals for **2**-d_5 appear as singlets (^{2}H{^{1}H}NMR), these resonances are broad, and it is, therefore, possible that this is a coupled system in which the fine structure is not resolved. If this is indeed the case, the equation used to calculate k_1 which assumes uncoupled systems will not be exact for this system. However, the error in application of this equation to coupled systems will depend in part on the magnitude of the coupling constants:[23] since we cannot resolve the couplings, the values are presumed to be small and, thus, use of this method to determine k_1 for **2**-d_5 is believed to be valid. (b) The error bars given for $k_1^{105°C}$ for **2** include possible values of k_1 for the temperature range 105 ± 5 °C.

the olefin hydride complexes can be determined from the equilibrium constants for competitive binding of ethylene and propene or styrenes to the niobium center by including contributions from the free olefins to the overall equilibrium (eq 12). From these measurements, partial free energy surfaces can be constructed (Figures 6[39] and 7). These data have allowed us to develop a fairly detailed description of the ground and transition states for the olefin insertion process in the $Cp^*_2Nb(olefin)(H)$ system.

Rather surprisingly, no net electronic effect for styrene binding is observed for the ground state for complexes **5a–e** as measured by equilibrium 12. Substituent effects on styrene–metal binding have been studied in some detail for palladium(II) and platinum(II).[40–42] Electron-releasing and -withdrawing substituents have been shown to affect the metal–styrene bonding for Pd(II) and Pt(II) as manifested by differences in the metal–styrene binding constants.[40a,42] For Pd(II) and Pt(II), the energetic differences in styrene–metal binding on varying the styrene substituents are small, though not negligible, with electron-donating substituents stabilizing the metal styrene complex in most cases. Since Pd(II) and Pt(II) are considered good σ-acceptors, but poor π-donors, this stabilization is consequently attributable to σ effects.[40] In contrast, the $[Cp^*_2NbH]$ unit is a good π-donor (ν(CO) = 1870 cm^{-1} for $Cp^*_2Nb(H)(CO)$[14]). Therefore, it was anticipated that metal-donor/olefin-acceptor effects would contribute significantly to styrene binding to $[Cp^*_2NbH]$; that is, the largest binding constant would be observed for the most electron-withdrawing substituent CF_3 and the smallest binding constant for the most electron-donating substituent NMe_2. Consequently, the apparent insensitivity of styrene–niobium binding to variations in the *para* substituents is difficult to reconcile. Two possible explanations can be forwarded. (1) A net balancing of donor and acceptor effects occurs; i.e., $CH_2{=}CHC_6H_4NMe_2$ serves as a sufficiently better donor to compensate roughly for its poorer acceptor ability relative to $CH_2{=}CHC_6H_4CF_3$. (2) Steric interactions force the phenyl ring out of resonance. Models of the ground state for complexes **5a–e** suggest considerable steric interaction of the aryl ring with the cyclopentadienyl methyl groups when the aryl and coordinated olefin π-systems are parallel (in resonance). This steric crowding is relieved somewhat on twisting the aryl partially out of resonance so that the ring lies flat between the two η^5-C_5Me_5 ligands (see Note Added in Proof). In this case, small substituent effects on styrene binding would be expected because of the reduced resonance interaction between the aryl and olefin π-orbitals of the coordinated styrenes.

The ordering of the ground-state ethylene, propene, and styrene complexes is the result of both steric and electronic effects. On steric grounds, it would be expected that the substituted olefin complexes would be destabilized relative to the ethylene complex because of the greater steric demands of the methyl or phenyl substituent relative to hydrogen. The observed ground-state ordering for $Cp^*_2Nb(CH_2{=}CHR)(H)$ of R = Ph < H suggests that a compensating, stabilizing electronic effect is operating for the styrene complex. Indeed, the metal-donor/olefin-acceptor interaction is expected to be strengthened: phenyl is inductively electron-withdrawing relative to H[43] and charge may be delocalized into the phenyl group by resonance.

Scheme III

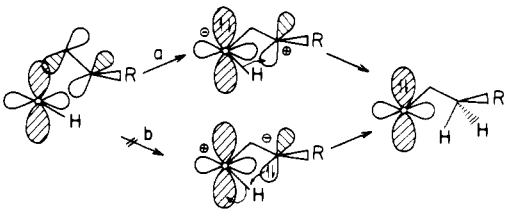

For this system, *it is seen that electron-donating substituents on the β carbon accelerate the rate of olefin insertion.* This observation suggests that partial positive charge is developed at the β carbon in the transition state. Lauher and Hoffmann have considered the correlation diagram for just such a bent metallocene, d^2 olefin hydride complex.[44] An important conclusion reached was that the electrons involved in metal-donor/olefin-acceptor bonding ($1a_1$ orbital) in the ground state correlate with the metal lone pair of the alkyl tautomer. In as much as the hydride–olefin insertion process involves breaking the metal-to-*endo* (β) carbon bond and making the hydride-to-β-carbon bond, two limiting cases for this transformation can be envisioned (Scheme III). In path a, the electron pair in the $1a_1$ orbital moves directly to the metal center in the metal-to-β-carbon bond-breaking process; the hydride ligand migrates to the carbon with its electron pair. In path b, the $1a_1$ electrons move to the p orbital on the β carbon in the metal–carbon bond breaking, with proton migration to the β carbon. Due to the low symmetry of this system, neither pathway is strictly forbidden on orbital symmetry grounds; however, path a is certainly in better agreement with our experimental findings, since for path a a partial positive charge on the endo (β) carbon in the transition state obtains.

Consequently, for the series of compounds studied, the electronic contributions to rate enhancement can be understood as follows. The transition state ordering R = H $\gtrsim$ Ph > Me for $CH_2{=}CHR$ insertion reflects the electronic properties of these substituents; both phenyl and methyl stabilize the developing positive charge at the β carbon in the transition state. Relative to H, methyl is inductively electron releasing[43] and, hence, transition-state stabilizing; phenyl is inductively electron withdrawing, yet electron releasing by resonance: the balance of these two effects leads to an overall small net stabilization of the styrene insertion transition state relative to ethylene.

The electronic effects of the para-substituted styrenes may be understood similarly. Substituents on the aryl ring contribute to charge stabilization or destabilization primarily by resonance. The reaction site (β-carbon) can be in direct resonance with the para substituent provided that the aryl ring is oriented such that its π-system can overlap with the p orbital on the β carbon. Correlation of the rate data (log k_1) with the Hammett constants σ_+ (direct resonance between X and reaction site) and σ_{para} (no direct resonance between X and reaction site) shows a better (albeit rather poor) linear fit to σ_{para} with ρ = −0.64 (Figure 5). This observation may be interpreted as indicating that a direct resonance interaction of the β carbon in the styrene insertion transition state with the aryl para substituent is minimal, perhaps due to twisting of the aryl ring to reduce unfavorable steric interactions with the pentamethylcyclopentadienyl ligand, as discussed for the ground state. Indeed, if, as suggested by these observations, direct resonance interaction of the olefin and aryl π-systems is not operating in both the transition and ground states, this description of the hydride–olefin insertion process is consistent with the aryl ring remaining out of resonance with the olefin π-system along the entire reaction coordinate due to the steric demands of the $[Cp^*_2Nb]$ ligand array.

(39) Thermodynamic data which allow assessment of contributions due to free styrenes for p-$XC_6H_4CH{=}CH_2$, X = Me_2N, MeO, or CF_3 are not available. Consequently, it is possible that any actual differences in the relative ground-state energies for these substituted styrenes are masked by compensating differences in stabilities of the free styrenes. Because of the modest difference in the correction ($^1/_2$(4.25 − 4.18) = 0.04 kcal mol^{-1}) to the relative binding energies for styrene and p-methylstyrene compared to the difference in their insertion barriers ($\Delta(\Delta G^*)$ = 0.1 kcal mol^{-1}), it is assumed that the relative ordering of the insertion rates for the substituted styrene complexes reflects the corresponding order of transition states (Figure 6). Furthermore, this assumption allows the development of a consistent explanation of the substituent effects on the transition state for hydride–olefin insertion.

(40) (a) Miki, K.; Shiotani, O.; Kai, Y.; Kasai, N.; Kanatani, H.; Kurosawa, H. *Organometallics* **1983**, *2*, 585–593. (b) Nyburg, S. C.; Simpson, K.; Wong-Ng, W. *J. Chem. Soc., Dalton Trans.* **1976**, 1865–1870.

(41) Cooper, D. G.; Hamer, G. K.; Powell, J.; Reynolds, W. F. *J. Chem. Soc., Chem. Commun.* **1973**, 449–450.

(42) (a) Ban, E.; Hughes, R. P.; Powell, J. *J. Organomet. Chem.* **1974**, *69*, 455–472. (b) Shupack, S. I.; Orchin, M. *J. Chem. Soc.* **1964**, 586–590.

(43) Lowry, T. H.; Richardson, K. S. "Mechanism and Theory in Organic Chemistry", 2nd ed.; Harper & Row Publishers: New York, 1981; pp 130–145, 205–212.

(44) Lauher, J. W.; Hoffmann, R. *J. Am. Chem. Soc.* **1976**, *98*, 1729–1742.

The relatively small ρ value observed for hydride–olefin insertion in this system is consistent with a cyclic transition state with little charge separation.[43] Likewise, the observation of no change in the styrene insertion barrier in solvents of varying polarity supports a largely nonpolar transition state. Consequently, although the description of the transition state developed in this study indicates the development of partial positive charge at the β-carbon and movement of the hydride more nearly as H^- than as H^+, the overall charge separation in the transition state must nonetheless be small as expected for concerted hydride–olefin insertion.

The kinetic isotope effect on hydride–olefin insertion for **2**-d_5 is measured as $k_H/k_D = 1.1 \pm 0.4$. Unfortunately, this number does not give any detailed information on the insertion transition-state geometry since it represents a composite isotope effect which is the product of a normal primary isotope effect and four inverse secondary isotope effects.[43] The secondary isotope effect involves an sp^2 to sp^3 hybridization change of two carbons each of which are bound to two deuteriums. The values of k_H/k_D for this type of secondary isotope effect generally range from 0.8 to 0.9.[43] Using these numbers, an estimated range for the primary isotope effect for hydride–olefin insertion in **2**-d_5 can be obtained. $(1.7 \pm 0.6) < k_H/k_D < (2.7 \pm 1.0)$. This range for the primary kinetic isotope effect for hydrogen transfer is inclusive of the values calculated and measured for related models involving a cyclic four-center transition state.[45]

Conclusions

For the Cp^*_2Nb(olefin)(H) system, we have seen that both steric and electronic effects operate in the ground-state olefin–hydride complex. In contrast, electronic effects dominate in the transition state for hydride–olefin insertion. In summary, the results of our study of the kinetics and mechanism of olefin insertion into the niobium hydride bond of Cp^*_2Nb(olefin)(H) support the generally proposed picture for olefin insertion and β-H elimination: insertion and elimination proceed through a relatively nonpolar, cyclic transition state with concerted bond making and bond breaking (eq 15). Furthermore, we have been able to show

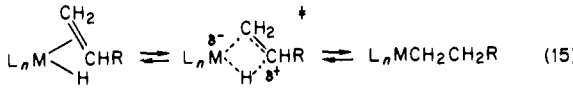

(15)

that fractional positive charge develops at the β-carbon in this transition state and that the hydrogen migrates more nearly as H^- than as H^+. We anticipate that this picture will describe the olefin insertion/β-H elimination step for other metal systems for which metal–hydrogen bonds are hydridic in character. Indeed, for the related reaction of substituted styrenes with 9-borabicyclo[3.3.1]nonane, relative rates of hydroboration gave a value of $\rho(\sigma^+) = -0.49$, consistent with a small buildup of positive charge on the substituted olefinic carbon ($CH_2{=}CHR$) and addition of the hydridic boron–hydrogen bond in the sense $B^{\delta+}$–$H^{\delta-}$.[46] Significantly, in Halpern and Okamoto's study of the reaction of substituted styrenes with $RhH_2Cl(PPh_3)_3$, the variation in the value of the hydride–olefin insertion rate constant with substituent ($\rho(\sigma^+) \cong -0.9$) is found to arise largely from differences in the stabilities of the ground states of the olefin complexes.[8c] It would be of considerable interest to establish whether these descriptions of the transition state hold true for olefin insertion into other metal–hydrogen bonds, including those which are more hydridic than Nb–H and more acidic than Rh–H.

Experimental Section

General Considerations. All manipulations were performed by using glovebox and high-vacuum line techniques. Solvents were dried over $LiAlH_4$ and stored over titanocene.[47] NMR solvents: benzene-d_6 and toluene-d_8 were dried over activated 4-Å molecular sieves and stored over titanocene; pyridine-d_5 and DMF-d_7 were stored over activated 4-Å molecular sieves; THF-d_8 was purified by vacuum transfer from sodium benzophenone ketyl.

Argon and hydrogen were purified by passage over MnO on vermiculite[48] and activated 4-Å molecular sieves. Ethylene (Matheson) and propene (Matheson) were purified by several freeze–pump–thaw cycles at −196 °C, then vacuum transferred at −78 and +25 °C, respectively. Styrene (Eastman), *p*-methylstyrene (Alfa), and *p*-methoxystyrene (Alfa) were used without further purification. *p*-(Trifluoromethyl)styrene was prepared by the literature method[49] except using the reaction of *p*-(trifluoromethyl)benzaldehyde (Marshallton) with MeMgBr to form the secondary carbinol $CF_3C_6H_4CH(OH)CH_3$. *p*-(Dimethylamino)styrene[50] was prepared by this same procedure from *p*-(dimethylamino)benzaldehyde (Aldrich). Both styrenes were purified by Kügelrohr distillation and identified by ^1H NMR. Carbon monoxide (Matheson) and ^{13}CO (MRC-Mound) were used directly from the cylinder. Methyl isocyanide, prepared by literature methods,[51] was stored over activated 4-Å molecular sieves. Ethyl- and *n*-propylmagnesium bromides were purchased from Aldrich as diethyl ether solutions and used as received. Ethyl-d_5 bromide (Stohler) was used as received. $Cp^*_2NbH_3$ (**1**) and $Cp^*_2NbCl_2$ (**3**) were prepared as previously described.[14]

NMR spectra were recorded on Varian EM390 (90-MHz ^1H), JEOL FX90Q (89.56-MHz ^1H, 22.50-MHz ^{13}C, 13.70-MHz ^2H, 84.26-MHz ^{19}F), and Bruker WM500 (500.13-MHz ^1H, 125.8-MHz ^{13}C) spectrometers. Infrared spectra were recorded on a Beckman 4240 spectrophotometer and are reported in cm^{-1}. Elemental analyses were determined by Alfred Bernhardt Analytical Laboratory, Galbraith Laboratory, Dornis and Kolbe Microanalytical Laboratory and the analytical facilities at Caltech.

Procedures. **$Cp^*_2Nb(CH_2{=}CH_2)(H)$ (2).** (a) Compound **2** was prepared as orange-yellow crystals in 95% yield from the reaction of **1** with ethylene as previously described.[14b] (b) **3** (0.12 g, 0.28 mmol) was placed in a flask with 5 mL of diethyl ether. A 0.25-mL (0.65 mmol) portion of EtMgBr (2.58 M) in diethyl ether was added by syringe to the solution at −78 °C. The reaction mixture was allowed to warm to 25 °C and was stirred for 1 h. The volatiles were removed under reduced pressure. The product was crystallized from petroleum ether to give 45 mg of yellow crystalline **2** (41%).

$Cp^*_2Nb(CH_2{=}CHMe)(H)$ (4). Procedure b was followed using **3** (1.0 g, 2.3 mmol) and 3.6 mL (7.2 mmol) of *n*-PrMgBr (2 M) in diethyl ether. The mixture was stirred at 25 °C for 7 h and yielded 0.65 g of orange-yellow crystalline **4** (69%). IR (Nujol): 3023, 1718, 1653, 1487, 1200, 1063, 1023, 933, 865, 716 cm^{-1}. Anal. Calcd for $C_{23}H_{37}Nb$: C, 67.97; H, 9.18. Found: C, 67.92; H, 9.20.

$Cp^*_2Nb(CH_2{=}CHPh)(H)$ (5a). Compound **1** (0.50 g, 1.4 mmol) was dissolved in 10 mL of toluene. A 0.60-mL portion (5.2 mmol) of styrene was added by syringe to the solution at −78 °C. The mixture was warmed to 90 °C and stirred for 12 h. The resulting yellow-brown solution was filtered and the volatiles were removed under reduced pressure. Crystallization from petroleum ether afforded 0.49 g of yellow crystalline **5a** (77%). IR (Nujol): 1743, 1679, 1592, 1484, 1223, 1169, 1142, 1067, 1024, 786, 742, 715, 695, 539 cm^{-1}. Anal. Calcd for $C_{28}H_{39}Nb$: C, 71.78; H, 8.39. Found: C, 72.40; H, 8.66.

$Cp^*_2Nb(CH_2{=}CHC_6H_4\text{-}p\text{-}NMe_2)(H)$ (5b). The above procedure was followed by using 0.98 g (2.7 mmol) of **1** and 1.2 mL (8.2 mmol) of *p*-(dimethylamino)styrene. Crystallization from petroleum ether yielded 1.00 g of yellow crystalline **5b** (73%). IR (Nujol): 3085, 3070, 3035, 1769, 1712, 1610, 1554, 1380, 1342, 1239, 1223, 1190, 1167, 1144, 1113, 1064, 1026, 948, 884, 824, 794, 748, 725, 532 cm^{-1}. Anal. Calcd for $C_{30}H_{44}NNB$: C, 70.43; H, 8.67; N, 2.74. Found: C, 70.38; H, 8.96; N, 2.78.

$Cp^*_2Nb(CH_2{=}CHC_6H_4\text{-}p\text{-}OMe)(H)$ (5c). The procedure used for the preparation of **5a** was followed by using 1.1 g (3.0 mol) of **1** and 1.2 mL (8.9 mmol) of *p*-methoxystyrene. Crystallization from petroleum ether yielded 1.5 g of yellow crystalline **5c** (53%). IR (C_6D_6): 1745, 1606, 1506, 1465, 1443, 1380, 1288, 1281, 1248, 1240, 1181, 1143, 1101, 1043, 1031, 863, 836, 730, 695, 648 cm^{-1}. Anal. Calcd for $C_{29}H_{41}NbO$: C, 69.89; H, 8.29; Nb, 18.64. Found: C, 70.10; H, 8.68; Nb, 18.29.

$Cp^*_2Nb(CH_2{=}CHC_6H_4\text{-}p\text{-}Me)(H)$ (5d). The procedure used for the preparation of **5a** was followed by using 0.80 g (2.2 mmol) of **1** and 1.0 mL (7.7 mmol) of *p*-methylstyrene. Crystallization from petroleum ether afforded 0.87 g of yellow crystalline **5d** (80%). IR (C_6D_6): 1738, 1606,

(45) More O'Ferrall, R. A. *J. Chem. Soc. B* **1970**, 785–790.
(46) Vishwakarma, L. C.; Fry, A. *J. Org. Chem.* **1980**, *45*, 5306–5308.
(47) Marvich, R. H.; Brintzinger, H. H. *J. Am. Chem. Soc.* **1971**, *93*, 2046.
(48) Brown, T. L.; Dickerhoof, D. W.; Bafus, D. A.; Morgan, G. L. *Rev. Sci. Instrum.* **1962**, *33*, 491.
(49) Baldwin, J. E.; Kapecki, J. A. *J. Am. Chem. Soc.* **1970**, *92*, 4869–4873.
(50) (a) Hall, H. K., Jr.; Dunn, L. C.; Padias, A. B. *J. Org. Chem.* **1980**, *45*, 835–838. (b) Marvel, C. S.; Overburger, C. G.; Allen, R. E.; Saunders, J. H. *J. Am. Chem. Soc.* **1946**, *68*, 736–738. (c) Strassburg, R. W.; Gregg, R. A.; Wallings, C. *Ibid.* **1947**, 2141–2143.
(51) Ugi, I.; Fetzer, U.; Enolzer, U.; Knupfer, H.; Offermann, K. *Angew. Chem., Int. Ed. Engl.* **1965**, *4*, 472.

1508, 1480, 1430, 1380, 1250, 1226, 1104, 1026, 863, 732, 680 cm^{-1}. Anal. Calcd for $C_{29}H_{41}Nb$: C, 72.18; H, 8.56. Found: C, 72.55; H, 8.42.

$Cp^*_2Nb(CH_2{=}CHC_6H_4$-*p*-$CF_3)(H)$ (5e). Compound **1** (0.79 g, 2.2 mmol) was dissolved in 10 mL of toluene. A 1.7-mL portion (9.9 mmol) of *p*-(trifluoromethyl)styrene was added by syringe to the solution at −78 °C. The mixture was allowed to warm slowly to 25 °C and was stirred at this temperature for 10 h. The volatiles were removed from the resulting orange solution under reduced pressure. Crystallization from petroleum ether afforded 0.90 g of bright yellow crystalline **5e** (78%). IR (Nujol): 1737, 1692, 1602, 1562, 1510, 1326, 1309, 1235, 1182, 1154, 1142, 1104, 1064, 1025, 1008, 951, 847, 844, 838, 800, 774, 732, 613, 591 cm^{-1}. Anal. Calcd for $C_{29}H_{30}F_3Nb$: C, 64.92; H, 7.14; F, 10.62; Nb, 17.32. Found: C, 64.80; H, 7.11; F, 10.41; Nb, 17.60.

$Cp^*_2Nb(Et)(CO)$ (6). A solution of **2** (1.0 g, 2.5 mmol) in 10 mL of toluene was stirred under 5 atm of CO in a glass bomb at 25 °C in the dark for 2 weeks. The volatiles and excess CO were removed from the resulting green solution under reduced pressured to yield a green solid. Recrystallization from petroleum ether at −78 °C afforded 0.92 g of blue crystalline **6** (86%). IR (C_6D_6): 1857, 1425, 1371, 1240, 1136, 1126, 1056, 1017, 852, 685 cm^{-1}. Anal. Calcd for $C_{23}H_{35}NbO$: C, 65.71; H, 8.39; Nb, 22.10. Found: C, 66.03; H, 8.19; Nb, 22.34.

$Cp^*_2Nb(CH_2CH_2Ph)(CO)$ (8a). The above procedure was followed by using 0.58 g (1.2 mmol) of **5a**; the mixture was stirred at 25 °C for 1 week. Recrystallization from petroleum ether afforded 0.44 g of bright green crystalline **8a** (72%). IR (C_6D_6): 1867, 1597, 1491, 1379, 1276, 1247, 1183, 1027, 861, 745, 697, 634 cm^{-1}. Anal. Calcd for $C_{29}H_{39}NbO$: C, 70.15; H, 7.92; Nb, 18.71. Found: C, 70.04; H, 7.91; Nb, 17.78.

$Cp^*_2Nb(Et)(CNMe)$ (10a). Compound **2** (0.55 g, 1.4 mmol) was dissolved in 20 mL of toluene in a flask equipped with a calibrated gas addition volume. Excess methyl isocyanide (6.7 mmol) was added by gas volume to the solution at −78 °C. The mixture was warmed to 25 °C and stirred for 3 days. The volatiles were removed from the resulting red solution to give a red solid. Recrystallization from petroleum ether afforded 0.25 g of bright red crystalline **10a** (41%). IR (Nujol): 1875, 1778, 1142, 1098, 1060, 1022, 940, 795, 718, 550 cm^{-1}. Anal. Calcd for $C_{24}H_{38}NNb$: C, 66.50; H, 8.84; N, 3.23. Found: C, 66.94; H, 9.10; N, 3.16.

$Cp^*_2Nb(CH_2CH_2Ph)(CNMe)$ (10c). The above procedure was followed by using 0.32 g (0.68 mmol) of **5a**. Recrystallization from petroleum ether afforded 0.16 g of red crystalline **10c** (46%). IR (Nujol): 1874, 1770, 1598, 1300, 1152, 1092, 1052, 1021, 937, 793, 749, 717, 693, 545 cm^{-1}. Anal. Calcd for $C_{30}H_{42}NNb$: C, 70.71; H, 8.31; N, 2.75. Found: C, 70.86; H, 8.15; N, 2.90.

Kinetics of Olefin Insertion Using Magnetization Transfer. ^1H NMR (500.13 MHz) magnetization-transfer experiments were performed on the Bruker WM500 spectrometer. Reaction temperatures were maintained by the WM500 temperature controller and were determined to be constant within ±1 °C by measuring the peak separation of an ethylene glycol sample before and after the experiments. Samples of recrystallized $Cp^*_2Nb(olefin)(H)$ complexes (~25 mg) in benzene-d_6 (0.4 mL) were sealed in NMR tubes under 700 torr of argon at −78 °C. The relaxation times for the protons of **2** and **5a–e** were measured for these samples at each temperature prior to performing the magnetization-transfer experiment using the inversion–recovery method[52] and analyzed with the WM500 three-parameter T_1 routine.[53] Magnetization-transfer spectra were obtained by using the DANTE pulsing technique[54] to invert a specific resonance, then delaying the $\pi/2$ observation pulse by a specified interval (t): $(n \times \pi/n)$–t–$\pi/2$ (with $n \sim 50$). Peak intensities were determined as ratios of the exchanging resonances to a constant resonance by cutting and weighing peak traces. A four-parameter nonlinear least-squares fit of the differences of the inverted resonance and the exchanging resonance as a function of delay time (t) to the magnetization equation was performed on a VAX computer by using a modified version of the program written by Perkin.[24] NOE difference spectra of exchanging signals for **2** and **5a** were measured by using the WM500 NOE routine[53] at 0 °C. No NOE enhancement of the hydride signals on saturating the exchanging olefin proton(s) signal or of the olefin proton(s) signal on saturating the hydride resonance was observed. Errors in k_1 were propagated from the standard deviation calculated for $k_{exchange}$ by the curve-fitting routine.

Kinetics of Olefin Insertion Using Coalescence Data. Coalescence of the two (η^5-C_5Me_5) resonances of compounds **4** and **5a–e** was observed in the ^1H NMR (89.56 MHz) at elevated temperatures. Samples were prepared as described above in sealed NMR tubes. The temperature at which coalescence occurred (T_c) was determined by measuring the peak separation of an ethylene glycol sample. Peak separation in the slow exchange limit ($\Delta\nu$) was measured at 25 °C. The equation $k_c = (\pi/(2^{1/2}))\Delta\nu$[23] was used to determine the rate constant at coalescence. $\Delta G^\ddagger$ was then calculated by using the Eyring equation, $\Delta G^\ddagger = RT \ln (KkT_c/k_ch)$,[23] assuming a transmission coefficient, $\kappa = 1$. Errors in k_c and $\Delta G^\ddagger$ represent approximately 1 standard deviation and were calculated from the estimated errors in measurement of T_c and $\Delta\nu$.

Calculation of Activation Parameters and Error Analysis. Arrhenius plots of $\ln k_1$ vs. $1/T$ were constructed from all data for **2** and **5a–e**. A nonweighted least-squares fit of the data for each compound to the Arrhenius equation $k_1 = \ln A - E_a/RT$[55] gave values of A and E_a. $\Delta H^\ddagger$ and $\Delta S^\ddagger$ were calculated from the equations $\Delta H^\ddagger = E_a - RT$ and $\Delta S^\ddagger = R \ln (ehA/k_BT)$. Values of $\Delta G^\ddagger$ calculated from $\Delta H^\ddagger - T\Delta S^\ddagger$ or from application of the Eyring equation ($\Delta G^\ddagger = RT \ln (\kappa kT/k_1h)$ assuming $\kappa = 1$) to the value of k_1 at 50 °C (interpolated or extrapolated from the Arrhenius plot) were identical.

Errors in E_A, A, $\Delta S^\ddagger$, $\Delta H^\ddagger$, and k_1 evaluated at 50 °C for **2** and **5b–e** represent 1 standard deviation calculated by error propagation of 1 standard deviation changes in the value of $-E_a/R$ and $\ln A$ when the measured k_1 values are varied within their error limits. Analysis of the residuals of the line gave smaller estimates of errors. In the case of **5a**, the standard deviations determined for the measured k_1 values were small compared to the scatter of the data about the least-squares line; therefore, the calculated variance, from analysis of residuals, was used as 1 standard deviation for the k_1 values and propagated into the values of the activation parameters. Standard deviations for $\Delta G^\ddagger$ evaluated at 50 °C were estimated from propagation of the $k_1^{50°C}$ error into the Eyring equation; errors in $\Delta G^\ddagger$ calculated from the errors in $\Delta H^\ddagger$ and $\Delta S^\ddagger$, including their covariance,[23] gave similar though somewhat smaller values.

Competitive Binding of Olefins to $[Cp^*_2NbH]$. Samples of **2** with excess propene or *para*-substituted styrenes, of **4** with ethylene and excess propene, and of **5a–e** with ethylene in benzene-d_6 in sealed NMR tubes were allowed to reach equilibrium at 25 °C. The equilibrium constants, $K_{eq} = [Cp^*_2Nb(CH_2{=}CHR)(H)][CH_2{=}CH_2]/[\mathbf{2}][CH_2{=}CHR]$, were calculated from peak intensities of the equilibrium mixture (^1H NMR) and $\Delta G = RT \ln K_{eq}$ was evaluated. The errors in K_{eq} and ΔG are estimated from standard deviations from the average of multiple determinations of K_{eq}.

$Cp^*_2Nb(CX_2{=}CX_2)(X)$ (2-d_m). The first procedure for preparing **2** was followed treating **1** (0.16 g, 0.44 mmol) with excess C_2D_4 (Stohler) (~2 mmol) in toluene at 100 °C for 12 h. **2**-d_m was recrystallized from petroleum ether yielding 0.06 g (35%). From the ^1H and ^2H NMR (C_6H_6) the ratios (hydride: β site:α site) were determined to be $H{:}H_\beta{:}H_\alpha$ = 1.00:1.07:1.17 and $D{:}D_\beta{:}D_\alpha$ = 1.00:2.45:2.50. From these ratios and the requirement that $(H+D){:}(H_\beta+D_\beta){:}(H_\alpha+D_\alpha)$ = 1:2:2, the empirical formula for this product is calculated as $(Cp^*_2\text{-}d_n)_2Nb(CH_{0.41}D_{1.63} = CH_{0.37}D_{1.59})(H_{0.35}D_{0.65})$ which can be described approximately as a mixture of 27 ± 7% $Cp^*_2\text{-}d_n)_2Nb\text{-}(CX_2{=}CD_2)(D)$, 35 ± 5% $(Cp^*_2\text{-}d_2)_2Nb(CX_2{=}CD_2)(H)$, and 38 ± 6% $(Cp^*_2\text{-}d_n)_2Nb(CX_2{=}CDH)(D)$.

$Cp^*_2Nb(CD_2{=}CD_2)(D)$ (2-d_5). The second procedure for preparing **2** was followed by using **3** (0.98 g, 2.3 mmol) and CD_3CD_2MgBr freshly prepared from CD_3CD_2Br (0.60 mL, 7.7 mmol) and excess Mg (0.52 g, 21.0 mmol). The mixture was stirred for 12 h at 25 °C and yielded 0.45 g (50%) of pale yellow 2-d_5 after recrystallization from petroleum ether. ^1H NMR (C_7D_8): δ 1.61 (s). ^2H NMR (14 MHz C_7H_8): δ 0.418 (s), −0.36 (s), −3.16 (s). IR (Nujol): 2293, 2204, 2188, 1487, 2338, 2060, 1024, 924, 800, 710, 450, 400 cm^{-1}.

Note Added in Proof. An X-ray diffraction study of the solid-state structure of $Cp^*_2Nb(CH_2{=}CHPh)(H)$ (**5a**) confirms the endo geometry. Important bond lengths (Å) include Nb–CH_2 (2.290 (4), Nb–CHPh (2.309 (4)), H_2C–CHPh (1.431 (5)), and Nb–H (1.75 (3)). Moreover, the phenyl ring is twisted 32° out of resonance with the olefin π-bond: Burger, B. J.; Trimmer, M. S.; Santarsiero, B. D.; Bercaw, J. E., manuscript in preparation.

Acknowledgment. This work was supported by the National Science Foundation (Grant No. CHE-8024869). The use of the

(52) Farrar, T. C.; Becker, E. D. "Pulse and Fourier Transform NMR"; Academic Press: New York, 1971; pp 20–22.

(53) DISNMRP, 1982, Version 820601, Bruker WM500 Manual.

(54) Morris, G. A.; Freeman, R. *J. Magn. Reson.* **1978**, *29*, 433–462.

(55) Some authors have stated that the Eyring equation, $\ln (k/T) = -\Delta H^\ddagger/RT + \Delta S^\ddagger/k + \ln (k_B/h)$, is a more general treatment of the temperature dependence of k. This equation has been used widely in the evaluation of kinetic data determined by NMR methods. However, use of the Eyring equation requires the assumption of a value of the transmission coefficient κ, usually set as $\kappa = 1$. Because of this assumption, we feel that Arrhenius equation is the more general and chose to use it in evaluation of the temperature dependence of k_1. In any case, it is noted that application of the Eyring equation to the data for **2** and **5a–e** yield values of $\Delta H^\ddagger$, $\Delta S^\ddagger$, $k_1^{50°C}$, and $\Delta G^\ddagger$ identical with those obtained by the Arrhenius treatment.

Southern California Regional NMR Facility, support by National Science Foundation Grant No. CHE-7916324, is also gratefully acknowledged. We thank Professors Dennis Dougherty, Robert Bergman, and Dr. Chris Roe for helpful discussions during the course of this work, and Professor Jack Halpern for a preprint of ref 8c.

Registry No. 1, 93558-77-1; **1**-d_3, 95313-85-2; **2**, 95313-60-3; **2**-d_5, 95344-20-0; **3**, 95313-61-4; **4**, 95313-62-5; **5a**, 95313-63-6; **5b**, 95313-64-7; **5c**, 95313-65-8; **5d**, 95313-66-9; **5e**, 95313-67-0; **6**, 95313-68-1; **7**, 95313-69-2; **8a**, 95313-70-5; **8b**, 95344-21-1; **8c**, 95313-71-6; **8d**, 95313-72-7; **8e**, 95313-73-8; **9**, 95344-22-2; **10a**, 95344-23-3; **10b**, 95313-74-9; **10c**, 95313-75-0; **10d**, 95313-76-1; **10e**, 95313-77-2; **10f**, 95313-78-3; **10g**, 95313-79-4; $Cp^*_2Nb(CH_2CH_3)$, 95313-80-7; $Cp^*_2Nb(CH_2CH_2CH_3)$, 95313-81-8; $Cp^*_2Nb(CH_2CH_2Ph)$, 95344-24-4; $Cp^*_2Nb(CH_2CH_2C_6H_4\text{-}p\text{-}NMe_2)$, 95313-82-9; $Cp^*_2Nb(CH_2CH_2C_6H_4\text{-}p\text{-}OMe)$, 95313-83-0; $Cp^*_2Nb(CH_2CH_2C_6H_4\text{-}p\text{-}Me)$, 95313-84-1; $Cp^*_2Nb(CH_2CH_2C_6H_4\text{-}p\text{-}CF_3)$, 95344-25-5; $Cp^*_2Nb(CD_2CD_3)$, 95313-86-3; C_2D_4, 683-73-8; $CD_3CD_2M_9Br$, 5780-97-2; CD_3CD_2Br, 3675-63-6; benzene-d_6, 1076-43-3; tetrahydrofuran-d_8, 1693-74-9; pyridine-d_5, 7291-22-7; dimethylformamide-d_7, 4472-41-7; ethene, 74-85-1; propene, 115-07-1; styrene, 100-42-5; *p*-(dimethylamino)styrene, 2039-80-7; *p*-methoxystyrene, 637-69-4; *p*-methylstyrene, 622-97-9; *p*-(trifluoromethyl)styrene, 402-50-6; 1-butene, 106-98-9; 2-butene, 107-01-7; poly(acrylonitrile), 25014-41-9; poly(*p*-chlorostyrene), 24991-47-7; acrylonitrile, 107-13-1; *p*-chlorostyrene, 1073-67-2; vinyl fluoride, 75-02-5.

Supplementary Material Available: An appendix containing a description of the physical basis for the magnetization trans transfer experiment, the FORTRAN program used for nonlinear least-squares analysis of the magnetication equation for chemical exchange, and the ^1H NMR data for the alkyl derivatives, $Cp^*_2Nb(CH_2CH_2R)(CO)$ (**8b-e**, **9**) and $Cp^*_2Nb(CH_2CH_2R)(CNMe)$ (**10b,d-g**) (15 pages). Ordering information is given on any current masthead page.

A Molecular Orbital Evaluation of Possible Factors Affecting the Homolytic Activation of Coenzyme B_{12}

David W. Christianson[†] **and William N. Lipscomb***

Contribution from Gibbs Chemical Laboratories, Department of Chemistry, Harvard University, Cambridge, Massachusetts 02138. *Received October 22, 1984*

Abstract: Utilizing the approximate ab initio method of partial retention of diatomic differential overlap (PRDDO), we have investigated the overlap population of the Co–C bond in a model system of coenzyme B_{12} after applying a variety of electronic perturbations. The results of the calculations show that electronically, the organocobalt linkage is particularly susceptible to angular distortion or steric crowding. However, the weakening of this linkage is not significantly advantaged by equatorial ligand "pucker" or a trans-electronic effect. It is therefore likely that steric interaction, probably causing the angular distortion of the Co–C bond, is primarily responsible for the weakening of the Co–C bond and its ultimate homolysis in actual B_{12} holoenzymes.

Coenzyme B_{12} is unique among biological molecules in that it contains a stable cobalt–carbon bond.[1] Furthermore, it is generally agreed that organometallic homolysis heralds the catalytic mechanism in enzymatic reactions dependent on the coenzyme.[2,3] However, the mode of activation of this dissociation under the relatively mild conditions of an enzymatic process remains a mystery, since the scission is only accomplished under nonphysiological conditions readily by photolysis. This activation could arise from steric crowding, electronic perturbations, or a combination of both effects induced upon the binding of coenzyme to apoenzyme or the binding of substrate to holoenzyme.

The observation that the corrinoid skeleton of coenzyme B_{12} is relatively flexible[4] has led to the suggestion that steric effects arising from its distortion are catalytically important. Such effects are demonstrably significant in the Co–C homolysis of model compounds. Halpern[5,6] has rationalized a relatively weak Co–C bond in coenzyme B_{12} on the basis of kinetic and thermodynamic studies on model compounds and also observed that steric interaction between the alkyl and equatorial ligands significantly decreases the dissociation energy. Indeed, Halpern and colleagues have recently determined the Co–C dissociation energy of the coenzyme itself to be 26 ± 2 kcal/mol and proposed that steric interaction between the 5′-deoxyadenosyl group and the corrinoid macrocycle are likely responsible for the bond-weakening effects.[7] Additionally, sterically crowded alkylcobalamines display an inherent instability likely arising from corrinoid distortion.[8] Studies of the coenzyme itself with modified peripheral groups indicate that these groups interact with the enzyme to facilitate the catalysis,[9] further suggesting that a conformational change in the corrinoid is catalytically significant. Such a conformational change could sterically induce a linear and/or angular distortion of the Co–C bond, resulting in its activation. Alternatively, such a conformational change could be catalytically significant in light of its perturbation of the stereoelectronic environment about the central cobalt ion. The ionic radius[10] of Co^{3+} is 0.63 Å, whereas that of Co^{2+} is 0.74 Å. During the course of homolysis, therefore, the corrinoid must be able to accommodate an increase in diameter of the cobalt ion of more than 0.2 Å. The corrinoid could distort to accommodate the larger ion; conversely, upon corrinoid distortion, perhaps accompanying the binding of coenzyme to apoenzyme, the $Co^{3+} \rightleftharpoons Co^{2+}$ transition might be advantaged through stereoelectronic effects of the ligands.

The role of the trans ligand to organometallic bonds in model compounds has received considerable speculation and study; the

[†] AT&T Bell Laboratories Scholar.

(1) For an excellent collection of reviews, see: Dolphin, D., Ed. "B_{12}"; Wiley-Interscience: New York, 1982.
(2) Babior, B. M. *Acc. Chem. Res.* **1975**, *8*, 376.
(3) Abeles, R. H.; Dolphin, D. *Acc. Chem. Res.* **1976**, *9*, 114.
(4) Glusker, J. P., ref 1, Vol. I, p 23.
(5) Halpern, J., ref 1, Vol. I, p 501.
(6) Halpern, J. *Acc. Chem. Res.* **1982**, *15*, 238.
(7) Halpern, J.; Sook-Hui, K.; Leung, T. W. *J. Am. Chem. Soc.* **1984**, *106*, 8317.
(8) Grate, J. H.; Schrauzer, G. N. *J. Am. Chem. Soc.* **1979**, *101*, 4601.
(9) Toraya, T.; Krodel, E.; Mildvan, A. S.; Abeles, R. H. *Biochemistry* **1979**, *18*, 417.
(10) Pauling, L. "The Nature of the Chemical Bond", 3rd ed.; Cornell University Press: Ithaca, 1960; p 518.

0002-7863/85/1507-2682$01.50/0